

# Constraints from Cosmic Rays to Tensor Dark Matter

Reunión Anual de la División de Partículas y Campos 2024

Haydee Hernández Arellano

[hydhernandez@gmail.com](mailto:hydhernandez@gmail.com)

5 al 7 de junio del 2024  
Ciudad de México

07 junio 2024

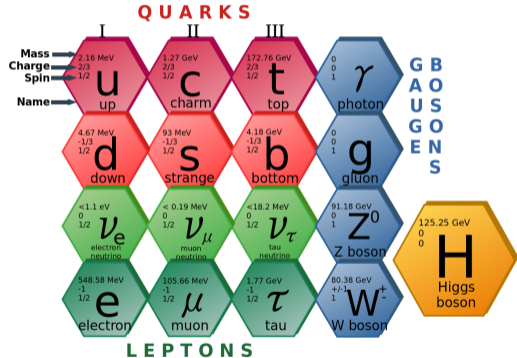


# Contenido

1. Introduction
2. Tensor Dark Matter
3. Relic Density
4. Direct Detection
5. Gamma-Ray Excess from the Galactic Center
6. Indirect Detection Constraints
7. Cosmic-Ray Antiproton Excess
8. Conclusions

# Standard Model

- Quantum Field Theory: Electromagnetic + Weak + Strong Forces
- Symmetry group:  $SU(3)_C \otimes SU(2)_L \otimes U(1)_Y$
- Self-consistent. Free of anomalies. Consistent perturbative scheme for systems at very high energies (LHC at 13 TeV)
- Higgs: last piece of the theory discovered in 2012,  $M_H = 125 \text{ GeV}$ .



## Dark matter: observational evidence

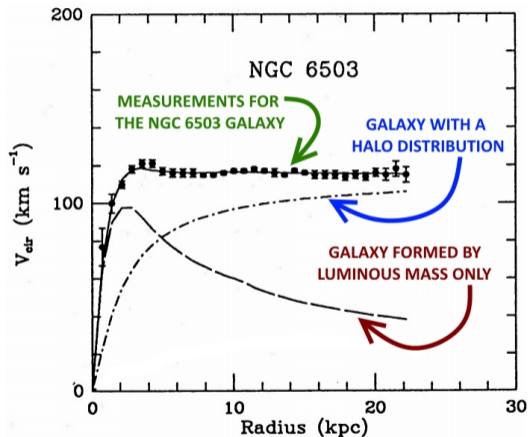


Figura: Rotation curve for the galaxy NGC6503 (Doroshkevich et. al., 2012).

## Dark matter: observational evidence

The strongest argument for the existence of DM is the observation of the cosmic microwave background (CMB).

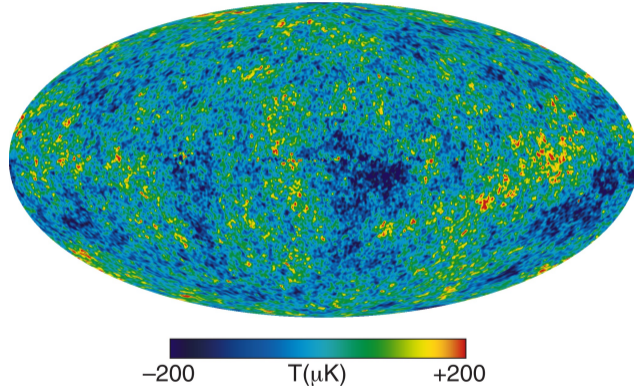
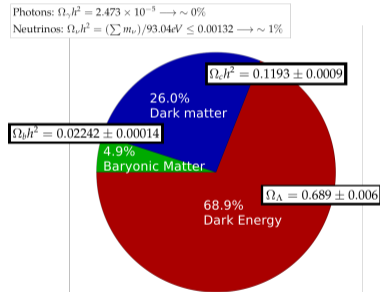


Figura: Internal Linear Combination Map (ILC), which is a linear combination of the WMAP (Wilkinson Microwave Anisotropy Probe) maps, at five different frequencies. This map shows the anisotropy of the CMB. (Bennett et. al., 2013).

## Dark matter: observational evidence

Fixing Planck's data:  $\Lambda$ CDM scheme + CMB anisotropies + baryon acoustic oscillations (BAO) distance measurements + Planck lensing (Planck 2018 results):

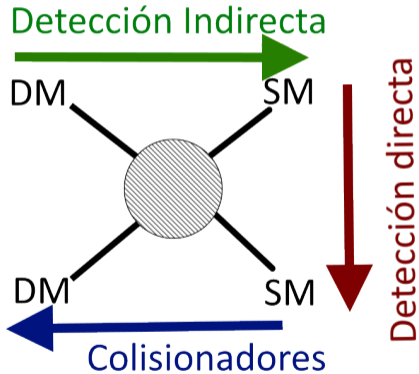
$$\begin{aligned} \rho_{\text{tot}}/\rho_c &\equiv \Omega_{\text{tot}} \equiv \sum_i \Omega_i + \Omega_\Lambda \\ &= 0.9993 \pm 0.0019. \end{aligned} \quad (1)$$



## Dark Matter Properties

- Relic density observed:  $\Omega_c h^2 = 0.1193 \pm 0.0009$ .
- Cold: non-relativistic before the matter dominated era to form the cosmological structures we see today. *Hot dark matter* is not sufficient to account for the DM content of the Universe. *Warm dark matter* is a possibility.
- Effectively neutral: interact very weakly with electromagnetic radiation. Effectively a singlet of the  $SU(3)_C \otimes SU(2)_L \otimes U(1)_Y$  group.
- Leave stellar evolution and Big Bang Nucleosynthesis predictions unchanged. The Tully-Fisher relation is another strong cosmological constraint.
- Consistent with current experimental bounds.

## Dark Matter Searches

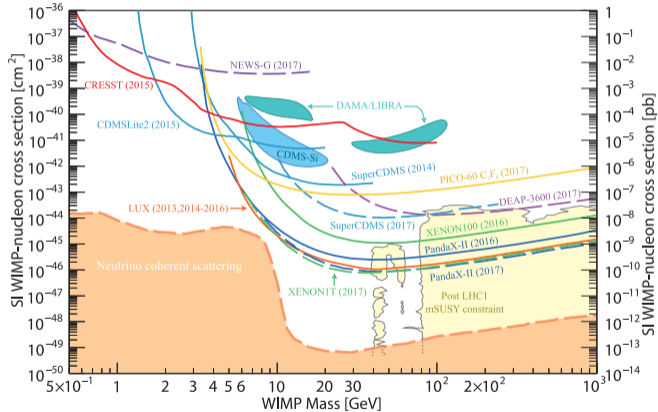


DM search approaches:

- Model based (*WIMPs, axion, ...*)
- Signal based (*fuzzy DM, astrophysics...*)

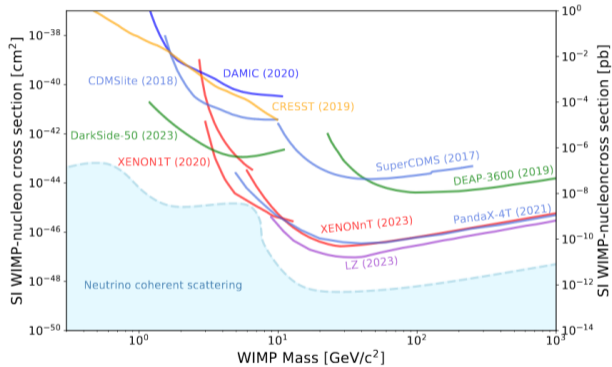


# Direct DM searches - 2018

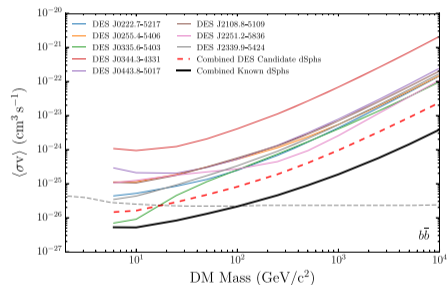


Particle Data Group, Phys. Rev. D. 2018.

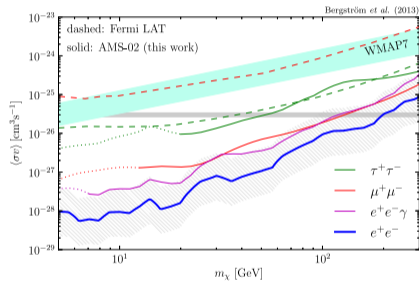
## Direct DM searches - 2023



## Indirect searches

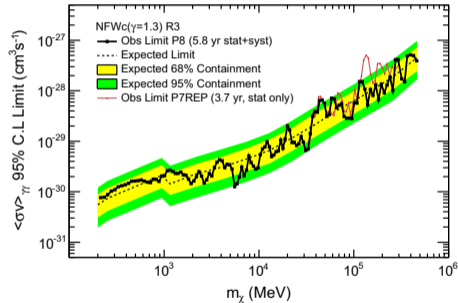


FermiLAT-DES, (APJ809, L4, 2015).

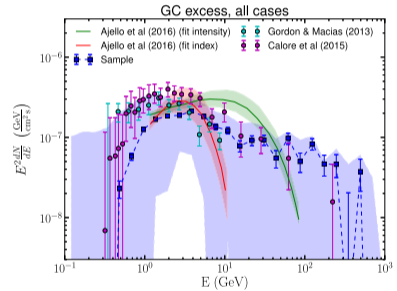


PRL111, 171101(2013) from AMS02 data.

## Indirect searches



FermiLAT: gamma rays from the GC (PRD91,122002 (2015), APJ840,43 (2017)).



## DM Candidates

Not a particle: Modified Newtonian Dynamics (MOND).

A particle:

- Sterile neutrinos: similar to the SM neutrinos, but without weak interactions.
- Axions: introduced as an attempt to resolve the strong CP problem.
- Supersymmetry particles: neutralinos, sneutrinos, gravitinos, axinos.
- Weak Interactive Massive Particle (WIMP).

## WIMP Paradigm

- Typical weak-scale pair-annihilation cross sections ( $\sigma \sim G_F^2 T^2$ ) for typical freeze-out temperatures ( $T \sim M/20$ ) and electroweak-scale masses ( $M \sim 100\text{GeV}$ ) produce a *thermal relic density* ( $\langle\sigma v_r\rangle \sim 10^{-26}\text{cm}^3\text{seg}^{-1}$ ), consistent with  $\Omega_c h^2 = 0.1193$ .
- Scheme that points to possible weak interactions of DM at electroweak scale (possible unified description of SM and DM?).
- Recent studies conclude that experimental bounds leave little room for this mass-cross section range (Arcadi et. al., *The Waning of the WIMP?*, 2018).

## Homogeneous Lorentz Group Irreps

The SM fields that describe matter and energy transform in the irreducible representations of the Homogeneous Lorentz Group (HLG): Causality + Locality + Poincaré invariance of the S-matrix...

$HLG \simeq SU(2)_A \otimes SU(2)_B \Rightarrow$  irreps classified according to two  $SU(2)$  quantum numbers.

Parity invariance: **Parity** maps  $(a, b) \leftrightarrow (b, a)$ . Invariance allows for irreps of the form:  $(a, a)$  or  $(a, b) \oplus (b, a)$ .

$$\begin{array}{cccccc}
 & & & & & (0, 0) \\
 & & & & & \\
 & & & & & (\frac{1}{2}, 0) \quad (0, \frac{1}{2}) \\
 & & & & & \\
 & & & & & (1, 0) \quad (\frac{1}{2}, \frac{1}{2}) \quad (0, 1) \\
 & & & & & \\
 & & & & & (\frac{3}{2}, 0) \quad (1, \frac{1}{2}) \quad (\frac{1}{2}, 1) \quad (0, \frac{3}{2}) \\
 & & & & & \\
 (2, 0) & (\frac{3}{2}, \frac{1}{2}) & (1, 1) & (\frac{1}{2}, \frac{3}{2}) & (0, 2) & 
 \end{array}$$

## Homogeneous Lorentz Group Irreps

The SM fields that describe matter and energy transform in the irreducible representations of the Homogeneous Lorentz Group (HLG): Causality + Locality + Poincaré invariance of the S-matrix...

$HLG \simeq SU(2)_A \otimes SU(2)_B \Rightarrow$  irreps classified according to two  $SU(2)$  quantum numbers.

Parity invariance: **Parity** maps  $(a, b) \leftrightarrow (b, a)$ . Invariance allows for irreps of the form:  $(a, a)$  or  $(a, b) \oplus (b, a)$ .

	Higgs	$(0, 0)$	
Quarks and Leptons	$(\frac{1}{2}, 0) \oplus (0, \frac{1}{2})$		
Gauge bosons	$(1, 0)$	$(\frac{1}{2}, \frac{1}{2})$	$(0, 1)$
Gravitino	$(\frac{3}{2}, 0)$	$(1, \frac{1}{2}) \oplus (\frac{1}{2}, 1)$	$(0, \frac{3}{2})$
Graviton	$(2, 0)$	$(\frac{3}{2}, \frac{1}{2})$	$(1, 1)$ $(\frac{1}{2}, \frac{3}{2})$ $(0, 2)$



## Homogeneous Lorentz Group Irreps

The SM fields that describe matter and energy transform in the irreducible representations of the Homogeneous Lorentz Group (HLG): Causality + Locality + Poincaré invariance of the S-matrix...

$HLG \simeq SU(2)_A \otimes SU(2)_B \Rightarrow$  irreps classified according to two  $SU(2)$  quantum numbers.

Parity invariance: **Parity** maps  $(a, b) \leftrightarrow (b, a)$ . Invariance allows for irreps of the form:  $(a, a)$  or  $(a, b) \oplus (b, a)$ .

$$\begin{array}{c}
 (0, 0) \\
 (\frac{1}{2}, 0) \oplus (0, \frac{1}{2}) \\
 \text{Our proposal } (1, 0) \oplus (0, 1) \\
 (\frac{3}{2}, 0) \quad (1, \frac{1}{2}) \oplus (\frac{1}{2}, 1) \quad (0, \frac{3}{2}) \\
 (2, 0) \quad (\frac{3}{2}, \frac{1}{2}) \quad (1, 1) \quad (\frac{1}{2}, \frac{3}{2}) \quad (0, 2)
 \end{array}$$

## Tensor Dark Matter: $(1, 0) \oplus (0, 1)$

In the HLG representations, the  $(1, 0) \oplus (0, 1)$  is associated with the **antisymmetric rank-2 Lorentz tensor** that describes the electromagnetic field:

$$F^{\mu\nu} = \partial_\mu A_\nu - \partial_\nu A_\mu.$$

We can take this approach: see **Phys. Rev. D85 (2012) 116006 [arXiv:1204.5337]**.

...However, it becomes much easier to work instead with a field represented by a  $2 \times (2j + 1)$  component spinor and work in the same approach as the Dirac fields.

## Dirac Fermions: $(\frac{1}{2}, 0) \oplus (0, \frac{1}{2})$

For the  $j = 1/2$  case:

The two  $SU(2)$  generators are:

$$A = \frac{1}{2}(J + iK), \quad B = \frac{1}{2}(J - iK), \quad (2)$$

where

$$J = \begin{pmatrix} \boldsymbol{\tau} & 0 \\ 0 & \boldsymbol{\tau} \end{pmatrix}, \quad K = \begin{pmatrix} i\boldsymbol{\tau} & 0 \\ 0 & -i\boldsymbol{\tau} \end{pmatrix}, \quad (3)$$

where  $\boldsymbol{\tau} = \frac{1}{2}\boldsymbol{\sigma}$ , and  $\boldsymbol{\sigma}$  are the Pauli matrices. The matrix form of a rotation and a boost in this case are

$$\mathcal{D}(\boldsymbol{\theta}) = e^{-i\mathbf{J}\cdot\boldsymbol{\theta}} = \cos\frac{\theta}{2} - i(\boldsymbol{\sigma}\cdot\mathbf{n})\sin\frac{\theta}{2}, \quad (4)$$

$$\mathcal{B}_{R/L}(\boldsymbol{\phi}) = e^{i\mathbf{J}\cdot\boldsymbol{\phi}} = \cosh\frac{\phi}{2} \pm (\boldsymbol{\sigma}\cdot\mathbf{n})\sinh\frac{\phi}{2}. \quad (5)$$

## Dirac Fermions: $(\frac{1}{2}, 0) \oplus (0, \frac{1}{2})$

The parity operator  $\Pi$  is such that the generators transform as

$$\Pi J \Pi^{-1} = J, \quad \Pi K \Pi^{-1} = -K, \quad (6)$$

which in this base is  $\Pi = \begin{pmatrix} 0 & 1 \\ 1 & 0 \end{pmatrix}$ . In the rest-frame,  $\Psi(0)$  is an eigenstate under parity with eigenvalues  $\pi = \pm 1$ , satisfying

$$\frac{1}{2}(1 \pm \Pi)\Psi(0) = \Psi(0). \quad (7)$$

Performing a boost on both sides of the equation, we have

$$\begin{pmatrix} -\pi & \frac{E+\sigma \cdot p}{m} \\ \frac{E-\sigma \cdot p}{m} & -\pi \end{pmatrix} \Psi(p, \lambda) = 0, \quad (8)$$

which after some work becomes the well-known Dirac Equation

$$(\gamma^\mu \partial_\mu \mp m)\Psi(x) = 0, \quad (9)$$

where  $\gamma^\mu$  are the Dirac (gamma) matrices.

## Covariant basis for $(\frac{1}{2}, 0) \oplus (0, \frac{1}{2})$ representation

The decomposition external product of states indicates the rep. of the operators of the basis:

$$[(1/2, 0) \oplus (0, 1/2)] \otimes [(1/2, 0) \oplus (0, 1/2)] = (0, 0)_2 \oplus (1, 0) \oplus (0, 1) \oplus (1/2, 1/2)_2.$$

We identify :

- Two Lorentz scalar operators  $\rightarrow (0, 0)$ : the identity 1 and the chirality operator  $\gamma^5$ .
- Six operators  $\rightarrow (1, 0) \oplus (0, 1)$ : the group generators  $\sigma_{\mu\nu} = \frac{i}{2}[\gamma_\mu, \gamma_\nu]$ .
- Two traceless symmetric tensors  $\rightarrow (1/2, 1/2)$ :  $\gamma^\mu$  and  $\gamma^5\gamma^\mu$ .

FOR MORE DETAILS AND EXPLICIT CALCULATION UP TO  $j=3/2$  REFER TO: S. Gómez-Ávila and M. Napsuciale. *Phys. Rev. D* **88** (2013) 096012.

## The $(1, 0) \oplus (0, 1)$ representation: TENSOR DARK MATTER

Decomposition of the external product of states:

$$[(1, 0) \oplus (0, 1)] \otimes [(1, 0) \oplus (0, 1)] = (0, 0)_2 \oplus (1, 1)_2 \oplus (1, 0) \oplus (0, 1) \oplus (2, 0) \oplus (0, 2)$$

For  $(1, 0) \oplus (0, 1)$  the basis for operators is given by the following set of  $6 \times 6$  covariant matrices:

- 1  $\mathbb{I}$ , identity matrix (1)  $((0, 0))$ .
- 2  $\chi$ , chirality operator (1)  $((0, 0))$ .
- 3  $S^{\mu\nu}$ ,  $\chi S^{\mu\nu}$  symmetric traceless tensors (9+9).  $((1, 1))$
- 4  $M^{\mu\nu}$ , HLG generators (6)  $((1, 0) \oplus (0, 1))$ .
- 5  $C^{\mu\nu\alpha\beta}$ , antisymmetric under  $\alpha \leftrightarrow \beta$  or  $\mu \leftrightarrow \nu$ ; symmetric under  $(\alpha, \beta) \leftrightarrow (\mu, \nu)$ . Satisfies Bianchi identity (10)  $((2, 0) \oplus (0, 2))$ .

FOR MORE DETAILS AND FULL DISCUSSION SEE: M. Napsuciale, S. Rodríguez, R. Ferro-Hernández and S. Gómez *Phys. Rev. D* **93** (2016) 7, 076003.

## The $(1, 0) \oplus (0, 1)$ representation: TENSOR DARK MATTER

In a similar way, the rest-frame parity equation is:

$$\tilde{\mathbb{P}}_{\pm} \psi(0) = \frac{1}{2}(1 \pm \Pi)\psi(0) = \psi(0) \quad (10)$$

We can perform the boost and obtain

$$(S^{\mu\nu} \partial_{\mu} \partial_{\nu} + m^2)\psi(x) = 0. \quad (11)$$

Multiplying on the left by  $S^{\mu\nu} \partial_{\mu} \partial_{\nu} - m^2$  gives  $(\partial^4 - m^4)\psi(x) = 0 \rightarrow$  tachyonic solutions!

To avoid this we use the correct parity projectors for the general off-shell case:  $\mathbb{P}_{\pm}(p) = \frac{1}{2}(1 \pm \frac{S(p)}{p^2})$  and take the projection over the desired Poincaré orbit:

$$\frac{p^2}{m^2} \mathbb{P}_{\pm}(p) = \frac{1}{2m^2}(p^2 \pm S(p)), \quad (12)$$

and performing a boost yields the following equation

$$\left[ \frac{1}{2}(g^{\mu\nu} + S^{\mu\nu})\partial_{\mu} \partial_{\nu} + m^2 \right] \Psi(x) = 0$$

## Free Lagrangian

- The free Lagrangian for tensor dark matter (TDM) fields is given by,

$$\mathcal{L} = \partial_\mu \bar{\Psi} \Sigma^{\mu\nu} \partial_\nu \Psi - m^2 \bar{\Psi} \Psi$$

where  $\Sigma^{\mu\nu} = \frac{1}{2}(g^{\mu\nu} + S^{\mu\nu})$  and the field  $\Psi$  is a six component "spinor":  $\Psi(x) = U(p, \lambda)e^{-iP \cdot x}$ ;  
 $\bar{\Psi} \equiv \Psi^\dagger S^{00}$ .

- The field can be decomposed into its chiral components

$$\Psi = \Psi_R + \Psi_L, \quad \Psi_R = \frac{1}{2}(1 + \chi)\Psi, \quad \Psi_L = \frac{1}{2}(1 - \chi)\Psi.$$

- We can decompose the Lagrangian into chiral components but it is not chiral-invariant in the massless limit.

$$\begin{aligned} \mathcal{L} = & \frac{1}{2}(\partial_\mu \bar{\Psi}_R S^{\mu\nu} \partial_\nu \Psi_R + \partial_\mu \bar{\Psi}_L S^{\mu\nu} \partial_\nu \Psi_L) \\ & + \frac{1}{2}(\partial^\mu \bar{\Psi}_R \partial_\mu \Psi_L + \partial^\mu \bar{\Psi}_L \partial_\mu \Psi_R) - m^2(\bar{\Psi}_R \Psi_L + \bar{\Psi}_L \Psi_R) \end{aligned}$$

- Chiral gauge interactions are not possible. Vector gauge interactions are permitted.

**Full details:** M. Napsuciale, S. Rodríguez, R. Ferro-Hernández and S. Gómez-Ávila, **Phys. Rev. D93 (2016) 076003** [arXiv:1509.07938].



## Effective Field Theory

- We consider TDM fields as SM singlets (no SM charges) with their own (dark) gauge group (DG).
- SM fields assumed as singlets of the Dark Group (no DG charges).
- The leading terms in the effective theory are

$$\mathcal{L}_{\text{int}} = \bar{\Psi}(g_s \mathbb{I} + ig_p \chi) \Psi \tilde{H} H + g_t \bar{\Psi} M_{\mu\nu} \Psi B^{\mu\nu} + \mathcal{L}_{\text{selfint}}(\Psi).$$

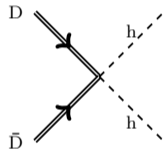
- In the unitary SM gauge, after SSB we get

$$\begin{aligned} \mathcal{L}_{\text{int}} = & \frac{1}{2} \bar{\Psi}(g_s \mathbb{I} + ig_p \chi) \Psi (v + h)^2 + g_t \cos\theta_W \bar{\Psi} M_{\mu\nu} \Psi F^{\mu\nu} \\ & - g_t \sin\theta_W \bar{\Psi} M_{\mu\nu} \Psi Z^{\mu\nu} + \mathcal{L}_{\text{selfint}}(\Psi) \end{aligned}$$

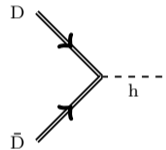
Further detail: H. Hernández-Arellano, M. Napsuciale and S. Rodríguez, **Phys. Rev. D98 (2018) 015001** [arXiv:1801.09853].

## TDM interactions with SM

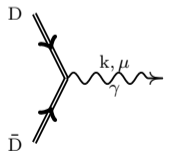
$$\mathcal{L}_{\text{int}}^{\text{SM}} = \frac{1}{2} \bar{\Psi} (g_s \mathbb{I} + i g_p \chi) \Psi (v + h)^2 + g_t \cos \theta_W \bar{\Psi} M_{\mu\nu} \Psi F^{\mu\nu} - g_t \sin \theta_W \bar{\Psi} M_{\mu\nu} \Psi Z^{\mu\nu} \quad (13)$$



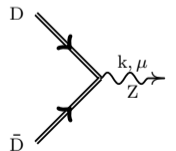
A Feynman diagram showing two incoming fermion lines, labeled D and  $\bar{D}$ , meeting at a vertex. Two outgoing dashed lines, labeled h, represent the higgs boson. The diagram is associated with the expression  $= i(g_s + i g_p \chi)$ .



A Feynman diagram showing two incoming fermion lines, labeled D and  $\bar{D}$ , meeting at a vertex. One outgoing dashed line, labeled h, represents the higgs boson. The diagram is associated with the expression  $= i(g_s + i g_p \chi)v$ .



A Feynman diagram showing two incoming fermion lines, labeled D and  $\bar{D}$ , meeting at a vertex. One outgoing wavy line, labeled  $\gamma$ , represents the photon. The momentum and index of the photon are labeled  $k, \mu$ . The diagram is associated with the expression  $= 2g_t \cos \theta_W M^{\mu\nu} k_\nu$ .



A Feynman diagram showing two incoming fermion lines, labeled D and  $\bar{D}$ , meeting at a vertex. One outgoing wavy line, labeled Z, represents the Z boson. The momentum and index of the Z boson are labeled  $k, \mu$ . The diagram is associated with the expression  $= -2g_t \sin \theta_W M^{\mu\nu} k_\nu$ .

## Dark matter relic density

- The measured dark matter relic density is

$$\Omega_D^{\text{exp}} h^2 = 0.1193 \pm 0.0009$$

- The evolution of the dark matter comoving number density  $n_D(T)$  is given by the Boltzmann equation

$$\frac{dY(x)}{dx} = -\frac{M^3 \langle \sigma v_r \rangle(x)}{H(M)} [Y^2(x) - Y_{\text{eq}}^2(x)]$$

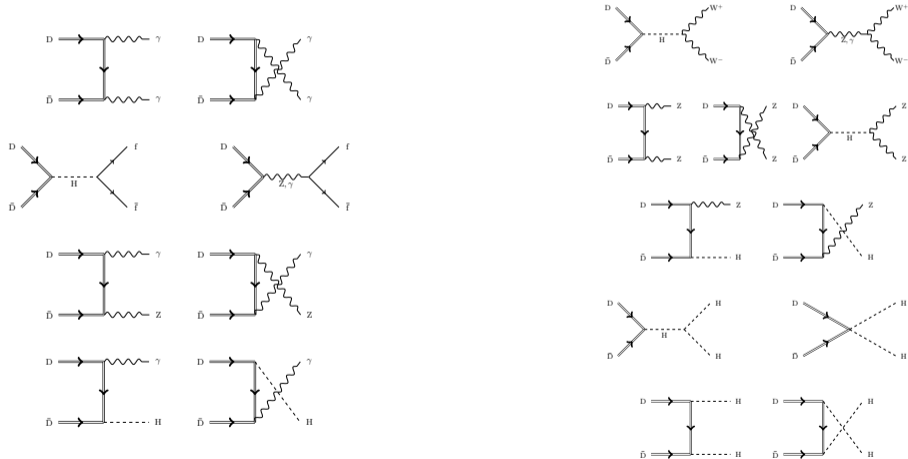
where  $M$  stands for the dark matter mass and

$$x \equiv \frac{M}{T}, \quad Y \equiv \frac{n_D}{T^3}, \quad H(M) = \frac{M^2 \sqrt{8\pi G_N g^*(M)}}{90}.$$

- Dark matter relic density is related to  $Y(x_0)$  by

$$\Omega_D = \frac{\rho_D(x_0)}{\rho_c} = \frac{M n_D(x_0)}{\rho_c} = \frac{M Y(x_0) T_0^3}{\rho_c}.$$

# Annihilation of TDM into SM particles



## TDM relic density for $M < M_H/2$

■  $D\bar{D} \rightarrow \gamma\gamma$ .

■  $D\bar{D} \rightarrow f\bar{f}$ , for  $m_f < M < M_H/2$ .

$$\langle\sigma v_r\rangle = \langle\sigma v_r\rangle_{\gamma\gamma} + \sum_f \langle\sigma v_r\rangle_{f\bar{f}} = a + 6b/x$$

with

$$a = \frac{29C_W^4 g_t^4}{18\pi M^2} + \sum_f \frac{N_f g_s^2 m_f^2 (M^2 - m_f^2)^{3/2}}{12\pi M^3 (M_H^2 - 4M^2)^2}$$

$$b = \frac{365C_W^4 g_t^4}{216\pi M^2} + \sum_f \frac{N_f \sqrt{M^2 - m_f^2}}{864\pi M^5} \left[ \frac{96M^4 g_t^2 M_Z^2 S_W^2 ((A_f^2 - 2B_f^2)m_f^2 + 2M^2(A_f^2 + B_f^2))}{v^2 (M_Z^2 - 4M^2)^2} + \frac{192A_f M^2 C_W Q_f g_t^2 M_W M_Z S_W^2 (m_f^2 + 2M^2)}{v^2 (M_Z^2 - 4M^2)} \right.$$

$$+ \frac{96C_W^2 Q_f^2 g_t^2 M_W^2 S_W^2 (m_f^2 + 2M^2)}{v^2} - \frac{6M^2 m_f^2 (8g_p^2 (4M^2 - M_H^2)(M^2 - m_f^2) + g_s^2 (-8m_f^2 (M^2 - M_H^2) - 11M^2 M_H^2 + 20M^4))}{(M_H^2 - 4M^2)^3}$$

$$\left. - \frac{9M^2 m_f^2 g_s^2 (4M^2 - 5m_f^2)}{(M_H^2 - 4M^2)^2} \right]$$

$$A_f = 2T_f^{(3)} - 4Q_f S_W^2, \quad B_f = -2T_f^{(3)}, \quad C_W = \cos \theta_W, \quad S_W = \sin \theta_W.$$

## Dark matter relic density

We need to evaluate  $Y(x_0 = M/T_0)$ , where  $T_0 = 2.7255(6) \text{ K} = 2.34865(52) \times 10^{-13} \text{ GeV}$  is the temperature of the cosmic background at the present.

For  $x > x_f$ , we have that  $Y(x) \gg Y_{\text{eq}}(x)$  and we can find an approximate solution by neglecting  $Y_{\text{eq}}(x)$  in the right hand side of the Boltzmann equation:

$$\frac{1}{Y(x_0)} = \frac{1}{Y(x_f)} + \sqrt{\frac{90}{8\pi^3 G_N}} M \int_{x_f}^{x_0} \frac{\langle \sigma v_r \rangle}{\sqrt{g_*(x)} x^2} dx. \quad (14)$$

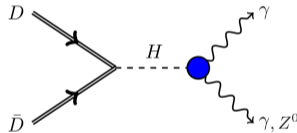
We can neglect the term  $Y(x_f)^{-1}$  to obtain the relic density

$$\Omega_{\text{DM}} h^2 = \frac{2T_0^3 h^2}{\rho_c} \sqrt{\frac{8\pi^3 G_N}{90}} \left( \int_{x_f}^{x_0} \frac{\langle \sigma v_r \rangle}{\sqrt{g_*(x)} x^2} dx \right)^{-1} \quad (15)$$

## Dark matter relic density: Complete Calculation

In the presence of resonances, the expansion can fail (K. Griest and D. Seckel, Phys. Rev. D43 (1991) 3191).

We also add SM one-loop level transitions:



$$\mathcal{L}_{\text{eff}} = H[G_{\gamma\gamma}F^{\mu\nu}F_{\mu\nu} + G_{Z\gamma}F^{\mu\nu}Z_{\mu\nu}], \quad (16)$$

where  $G_{\gamma\gamma}, G_{Z\gamma}$  are the corresponding form factors, which after being normalized can be written as  $G_{\gamma\gamma} = \frac{g_{\gamma\gamma}}{M_H}, G_{Z\gamma} = \frac{g_{Z\gamma}}{M_H}$ .

## Dark matter relic density: Complete Calculation

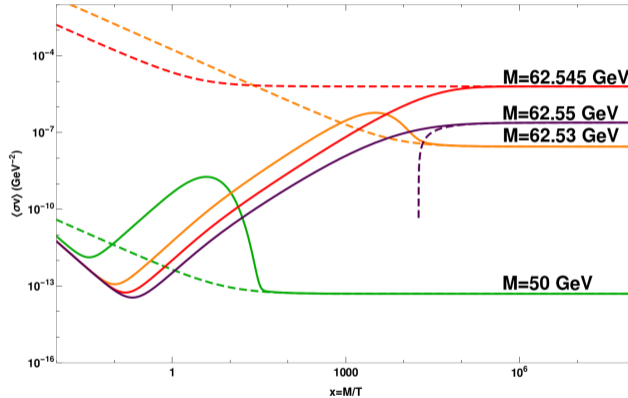


Figura: Thermal average cross-section (solid) and comparison with the non-relativistic expansion (dashed), for different values of the TDM mass.



## Dark matter relic density: Complete Calculation

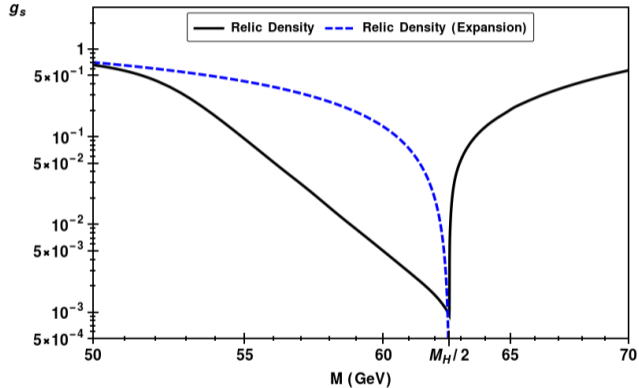
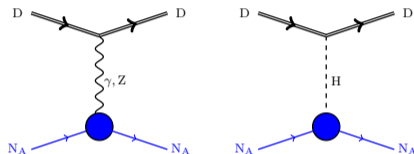


Figura: Values of the coupling  $g_s$  and TDM mass  $M$  consistent with the measured relic density near the Higgs resonance.

## Direct detection of Dark Matter



The rate of interactions of a DM particle of mass  $M$  with a nucleus of mass  $M_A$  in the detector is given by

$$\frac{dR}{dT} = \frac{\rho}{MM_A} \int_{v_{\min}}^{v_{\text{esc}}} |v| f(v) \frac{d\sigma}{dT}(T, v) d^3v,$$

where  $v_{\min}(T)$  is the minimal velocity of the incoming DM particle to produce a nuclear recoil energy  $T$ , and  $v_{\text{esc}} = 557 \text{ km/s}$  is the escape velocity in our galaxy.

## Nucleus-DM interactions: three layers of effective theory

The calculation occurs in three stages:

DM-Quarks  $\longrightarrow$  DM-Nucleons  $\longrightarrow$  DM-Nucleus

$$\mathcal{M} = \mathcal{M}_0 F(q^2), \quad (17)$$

where  $\mathcal{M}_0$  is the invariant amplitude calculated with the effective theory at the nuclear level and  $F(q^2)$  is the nucleus form factor.

The differential cross section using this terminology yields

$$\frac{d\sigma}{dT}(T, \nu) = \frac{|\bar{\mathcal{M}}_0(s, t, u)|^2}{32\pi M_A M^2 \nu^2} F^2(T). \quad (18)$$

## Nucleus-DM cross-section

Scattering takes place at low momentum transfer (low  $T$  in the LAB frame) and the XENON1T experiment, the detector is sensitive to  $T \in [3, 50]$  KeV. So we can write the actual differential cross section to leading order in  $T$  (in the dynamics) as

$$\frac{d\sigma}{dT}(T, v) = \frac{M_A}{2\mu_A^2 v^2} \left( \sigma_{SI} F_{SI}^2(T) + \sigma_{SD} F_{SD}^2(T) \right), \quad (19)$$

where  $\mu_A = M_A M / (M + M_A)$  is the DM-nucleus reduced mass.

In our case, we find that the **Spin-Independent** contributions are dominant. The corresponding cross-section is

$$\sigma_{SI} = \frac{\mu_A^2}{16\pi M_A^2 M^2} |\bar{\mathcal{M}}|^2(T_{\min}, v^2).$$

Assuming isospin conserving interactions, XENON1T report results in terms of the following observable

$$\sigma_P = \frac{\mu_P^2}{A^2 \mu_A^2} \sigma_{SI}.$$

We calculate  $\sigma_{SI}$  and normalize with the same factors to calculate XENON1T observable.

## Nucleus-DM cross-section: Expansion

$$|\bar{\mathcal{M}}|^2(T, v^2) = a_0 + \left( \frac{b_0}{T} + c_0 \right) v^2 + \mathcal{O}(T, v^4).$$

$$a_0 = \frac{4g_s^2 g_{\text{DN}_A \text{H}}^2 M_A^2}{m_{\text{H}}^4} + \frac{2g_{\text{DN}_A \gamma}^2}{3M^2} \left( M^2 - 2MM_A + 3M_A^2 \right) + \frac{16g_s g_{\text{DN}_A \gamma} g_{\text{DN}_A \text{H}} M_A^2}{3M m_{\text{H}}^2},$$

$$b_0 = \frac{4g_{\text{DN}_A \gamma}^2 M_A}{3},$$

$$c_0 = -\frac{16A_A g_{\text{DN}_A \gamma} g_{\text{DN}_A \text{Z}} M_A^2}{3M_{\text{Z}}^2} + \frac{8g_s g_{\text{DN}_A \gamma} g_{\text{DN}_A \text{H}} M_A^2}{3M m_{\text{H}}^2} - \frac{2g_{\text{DN}_A \gamma}^2 M_A}{3M^2} (M - 4M_A).$$

where

$$\begin{aligned} g_{\text{DN}_A \text{H}} &= -v g_{\text{HN}_A \text{N}_A}, \\ g_{\text{DN}_A \gamma} &= 2Z g_t \cos \theta_W, \\ g_{\text{DN}_A \text{Z}} &= \frac{M_{\text{Z}} g_t \sin \theta_W}{v}. \end{aligned}$$

## Nucleus-DM cross-section vs XENON1T data

The observable  $\sigma_p$  reported by XENON is given by

$$\sigma_p = \frac{1}{16\pi A^4 (M + M_p)^2} \left[ a_0 + \frac{b_0}{T_{\min}} v^2 + \mathcal{O}(T_{\min}, v^4) \right].$$

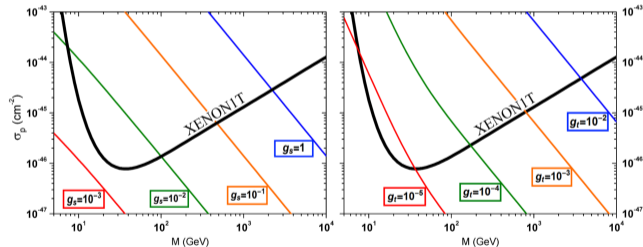


Figura: Observable  $\sigma_p$  as a function of the dark matter mass for the Higgs ( $g_t = 0$ , left panel) and spin ( $g_s = 0$ , right panel) portals, compared with the XENON1T upper bounds. We consider  $A = 129$ ,  $Z = 54$  and  $T_{\min} = 3$  KeV.

## Direct Detection: Final Results

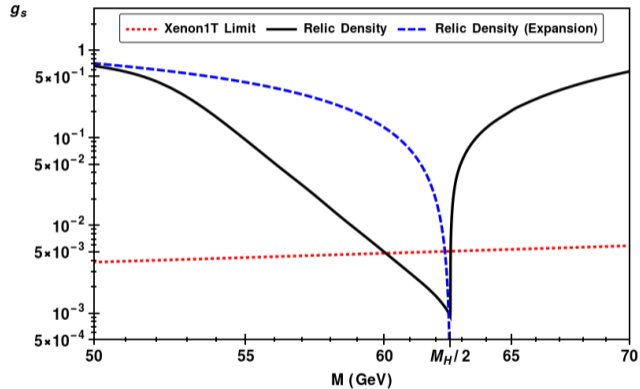
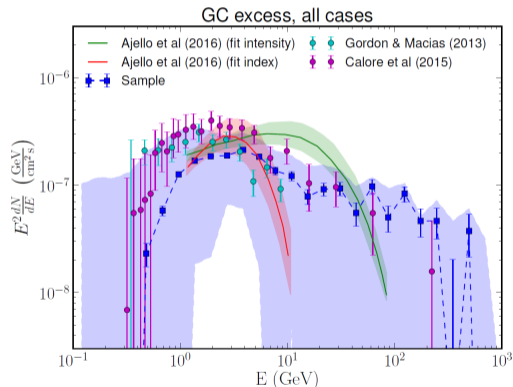


Figura: Full consistency for relic density and direct detection limits from XENON1T is obtained for  $M \in [60.056, 62.554]$  GeV.

## Gamma-Ray Excess in our Galactic Center

An excess in the gamma-ray flux from our Galactic Center has been claimed by several groups, centered around 3 GeV.



FermiLAT analysis: M. Ackermann et al., *Astrophys. J.* 840, 43 (2017).



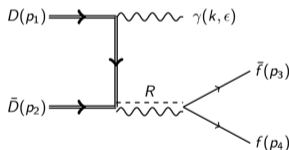
## Gamma-ray Differential Intensity

The GRE can be explained by some little known astrophysical sources, but **dark matter annihilation with photons in the final state** remains as an attractive possibility. Morphology of the emission consistent with this hipotesis.

■  $\bar{D}D \rightarrow X\gamma$ , with  $X = H, Z^0$

■  $\bar{D}D \rightarrow \gamma\gamma$

■  $\bar{D}D \rightarrow R\gamma \rightarrow \bar{f}f\gamma$ , with  $R = \gamma, H, Z^0, \bar{Q}Q[{}^{2S+1}L_J]$



The gamma-ray differential flux from annihilation of (not-self-conjugated) dark matter is

$$\frac{d\Phi}{d\omega} = \sum_i \frac{1}{4} \frac{B_i}{4\pi M^2} \frac{d\langle\sigma v_r\rangle_i}{d\omega} \left( \int_{\Delta\Omega} \int_{1.o.s} \rho^2(\vec{l}) dl d\Omega \right) \quad (20)$$

## GRE from DM annihilation into fermions

Several mechanisms have been proposed to explain the GRE.

- Delayed emission of secondary photons from **Bremsstrahlung or Inverse Compton Scattering (ICS)** of electrons from DM annihilation.  
*T. Lacroix, C. Boehm, and J. Silk, Phys. Rev. D90, 043508 (2014)..*
- GRE can be explained through  $\bar{D}D \rightarrow \bar{f}f$ , for  $M \in [5, 174]$  GeV,  
with  $\langle\sigma v_r\rangle \approx 10^{-26} \text{cm}^3/\text{seg} \equiv \langle\sigma v_r\rangle_{\text{thermal}}$ .  
*F. Calore, I. Cholis, C. McCabe, and C. Weniger, Phys. Rev. D91, 063003 (2015).*

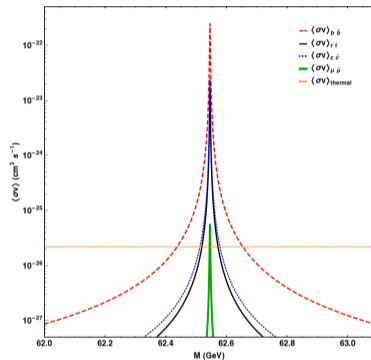
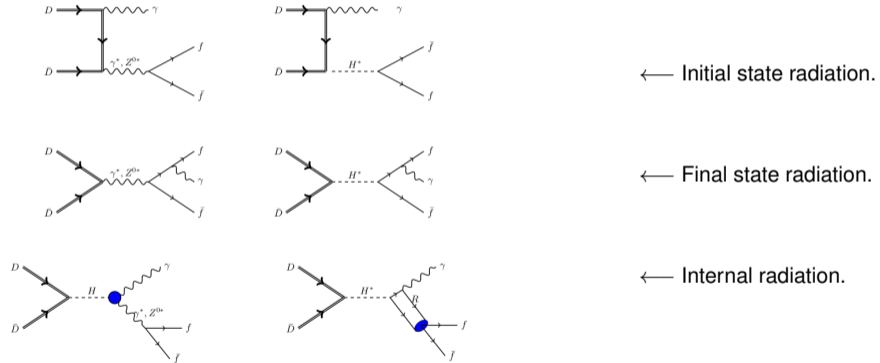


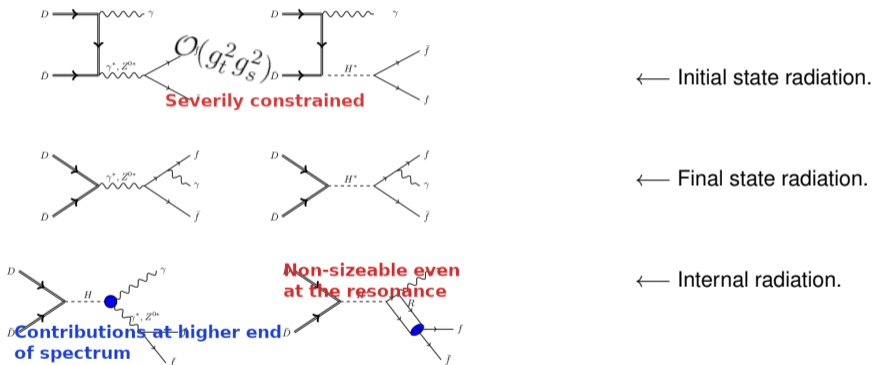
Figura: Cross-section of TDM annihilation into fermions for  $g_s = 2 \times 10^{-3}$ .

$$M \approx M_H/2$$

## GRE contributions from TDM



## GRE contributions from TDM



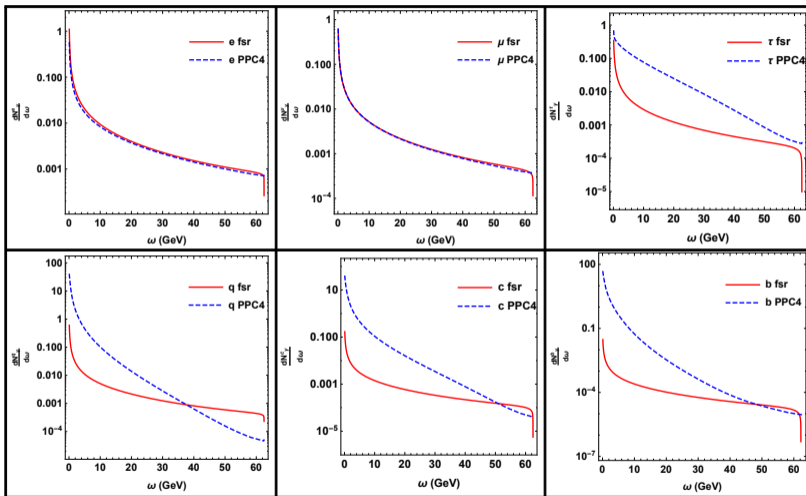
## Contributions to Prompt Photon Flux

Prompt photon production in FSR:

- Direct emission
- Decay products (leptons)
- Particle jets from hadronization of quarks

The last two modify our results for all fermions except for  $e$  and  $\mu$ , which do not have hadronic decays and are only affected by suppressed higher order EW radiative corrections.

We employ the packages of DarkSusy and PPC4DMID to calculate these fluxes, including radiative corrections.



Comparison of the direct photon emission versus the spectrum from PPC4DMID for  $M=62.5$  GeV.

## Prompt Photon Flux from TDM

The prompt photon flux contributions for  $g_s = 10^{-3}$  and  $M=62.49$  GeV. We use the gNFW profile with  $\gamma = 1.25$ , within a ROI with  $|l| < 10^\circ$  and  $2^\circ < |b| < 10^\circ$ , which yields a J-factor  $J_0 = 7.12 \times 10^5 \text{ GeV}^4/\text{cm}^2 \text{ seg}$ .

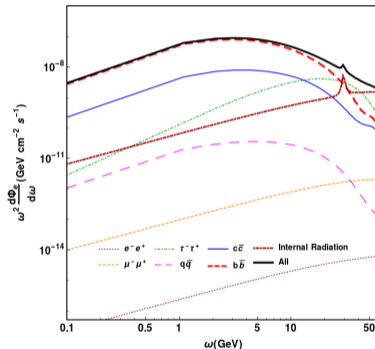


Figura: Differential flux for prompt photons and the internal radiation contribution.

## Delayed emission: Inverse Compton Scattering (ICS)

Delayed photon emission by ICS can be produced in at least three instances:

- Propagation of electrons produced in  $\bar{D}D \rightarrow e^+e^-$ .
- Propagation of electrons produced in decays of leptons or hadronization of quarks from  $\bar{D}D \rightarrow \bar{f}f$ .
- Propagation of muons produced in  $\bar{D}D \rightarrow \mu^+\mu^-$ .

These contributions were calculated with the NFW density profile since the PPC4DMID tabulated spectrum is designed for a number of profiles that don't include the gNFW. However, the contributions are not sensitive to the choice of density profile, so the results are compatible.



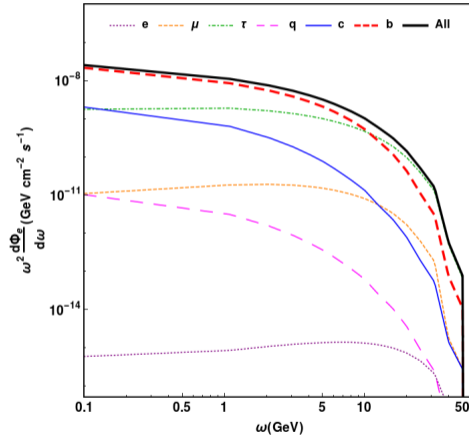
## Delayed emission: Inverse Compton Scattering (ICS)

Delayed photon emission by ICS can be produced in at least three instances:

- Propagation of electrons produced in  $\bar{D}D \rightarrow e^+e^-$ .  $\rightarrow$  Negligible due to small couplings.
- Propagation of electrons produced in decays of leptons or hadronization of quarks from  $\bar{D}D \rightarrow \bar{f}f$ .
- Propagation of muons produced in  $\bar{D}D \rightarrow \mu^+\mu^-$ .  $\rightarrow$  Three orders of magnitude below thermal cross section for this mass window.

These contributions were calculated with the NFW density profile since the PPC4DMID tabulated spectrum is designed for a number of profiles that don't include the gNFW. However, the contributions are not sensitive to the choice of density profile, so the results are compatible.

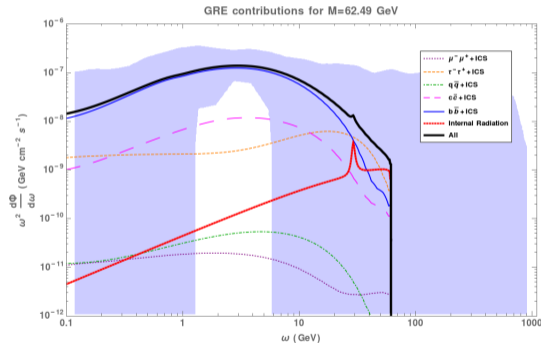
## ICS Flux from TDM



Contributions to the differential photon flux from ICS.

## GRE Contributions: Final Results

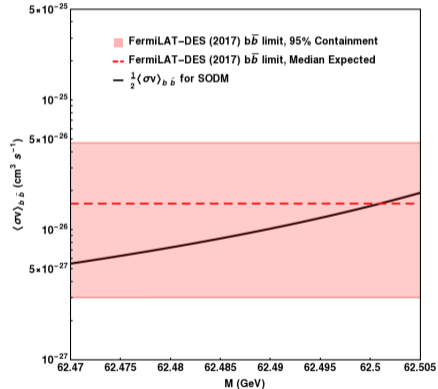
Considering the uncertainty band for the GRE obtained by FermiLAT, the values of  $g_s \in [0.98, 1.01] \times 10^{-3}$  and  $M \in [62.470, 62.505]$  GeV are consistent with the excess data.



Differential flux including all the contributions, for  $M=62.49$  GeV and  $g_s = 9.81 \times 10^{-4}$ .  
JHEP **08**, 106 (2020), doi:10.1007/JHEP08(2020)106 [arXiv:1911.01604 [hep-ph]].

## Other constraints: $\bar{b}\bar{b}$ limits

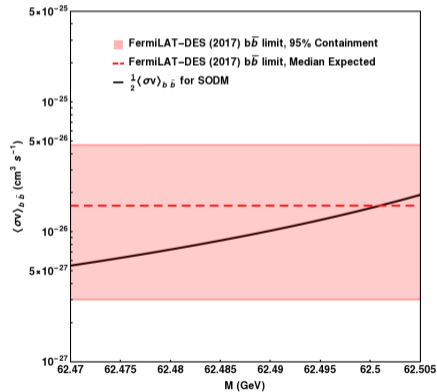
**Indirect detection:** Obtained from a combined analysis of the energy flux from 45 dwarf spheroidal galaxies (dSph).



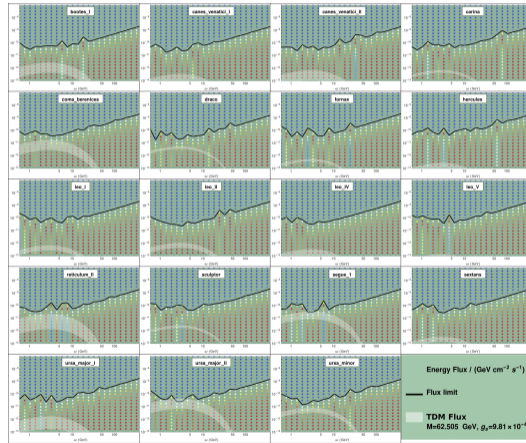
DES, Fermi-LAT collaboration, *Astrophys. J.* 809 L4 (2015). arXiv: 1503.02632.

## Other constraints: $\bar{b}b$ limits

**Indirect detection:** Obtained from a combined analysis of the energy flux from 45 dwarf spheroidal galaxies (dSph).  $\rightarrow$  Only 19 targets have a J-factor derived from experimental data on stellar dynamics (Astrophys. J. 801 (2015) 74. arXiv: 1408.0002.)



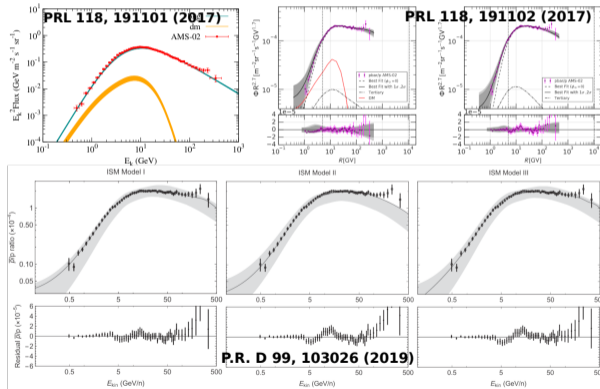
## Other constraints: Indirect detection in dSph galaxies



Bin-by-bin upper bound for the photon flux for the 19 targets, using the likelihood function data from *Astrophys. J.* 834 (2017) 110. [arXiv: 1611.03184](https://arxiv.org/abs/1611.03184).

## The AMS-02 data: Cosmic Ray Antiproton spectrum excess

There has been a number of reports of an excess of 10-20 GeV antiprotons observed at Earth. Studies seem to find that there is a consistency with DM annihilation when taking compatible values of  $M$  and  $\langle\sigma v\rangle$ .



- CR produced through hadronic interactions of high-energy protons and nuclei with interstellar gas.
- Injection and propagation of CR through the Galaxy modeled by solving the transport equation.
- There is also convection and diffusive reacceleration in the **interstellar medium** (ISM).
- CRs enter the Solar System and experience heliospheric forces → **Solar Modulation**.

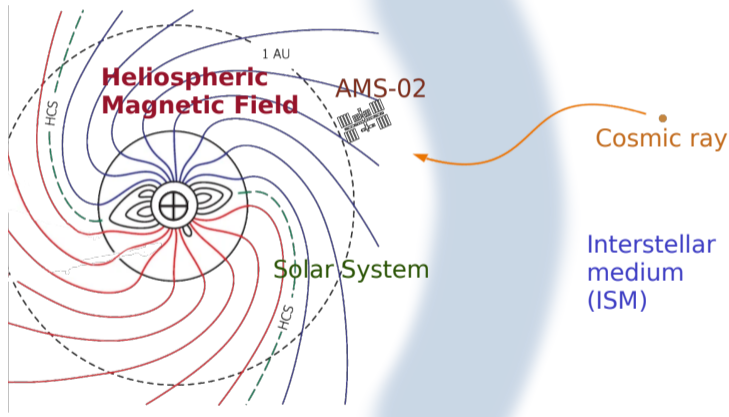


Figura: HMF diagram from Owens & Forsyth (2013).



## Modeling the production of antiprotons using GALPROP

- To model injection and propagation of CRs, we use the tool GALPROP, which takes care of solving the transport equation to yield the local flux of primary and secondary cosmic ray species.
- We adopt the models in Table I of Phys. Rev. D 99 103026 (Cholis et. al., 2019). We also find a combination of these parameters that best fit the new 2021 AMS-02 data, to get our Best-Fit configuration.

Parameter	Mod I	Mod II	Mod III	Best Fit
$\delta$	0.40	0.50	0.40	0.40
$z_L$ (kpc)	5.6	6.0	3.0	6
DM Core Radius (kpc)	0.0	20.0	0.0	20.0
DM local mass density ( $\text{GeVcm}^{-3}$ )	0.0	0.30	0.0	0.30
$D_0$ ( $\text{cm}^2\text{s}^{-1}$ )	$4.85 \times 10^{28}$	$3.10 \times 10^{28}$	$2.67 \times 10^{28}$	$4.85 \times 10^{28}$
$v_A$ (km/s)	24.0	23.0	22.0	24.0
$dv_c/d z $ (km/s/kpc)	1.0	9.0	3.0	1.0
$\alpha_1$	1.88	1.88	1.87	1.87
$\alpha_2$	2.38	2.45	2.41	2.38

Cuadro: Parameter configurations for the modeling of cosmic-ray propagation and injection in GALPROP.

## Production of antiprotons from Cosmic Rays

The cross section of the antiproton production is subject to uncertainties regarding its main sources:

- Inelastic collisions of high-energy nuclei. Studies focus on proton-proton collisions, and is well parametrized in different forms.
- Decay of antineutrons in the interstellar medium (ISM).
- Production from helium and other nuclei ( $\sim 40\%$  of the flux).

The  $3\sigma$  uncertainty on  $\sigma_{pp \rightarrow X + \bar{p}}$  was studied in Phys. Rev. D 90, 085017 (2014).

## Accounting for the uncertainties in the antiproton production

We employ the energy-dependent scaling factor used in Phys. Rev. D 95, 123007 (2017), to renormalize the flux:

$$N_{CS}(E_{kin}^{ISM}) = a + b \ln\left(\frac{E_{kin}^{ISM}}{\text{GeV}}\right) + c \left[\ln\left(\frac{E_{kin}^{ISM}}{\text{GeV}}\right)\right]^2 \quad (21)$$

The parameters  $a, b, c$  are bound so that the scaling factor resides within the uncertainty limit shown previously.

### Applying solar modulation:

The differential flux at Earth,  $dN^{\oplus}/dE_{kin}$  in terms of the kinetic energy of the particle in the ISM,  $k_{ISM}$  is

$$\frac{dN^{\oplus}}{dE_{kin}}(k_{ISM}) = \frac{(k_{ISM} - |Z|e\Phi(R) + m)^2 - m^2}{(k_{ISM} + m)^2 - m^2} \times \frac{dN^{ISM}}{dk_{ISM}}(k_{ISM}), \quad (22)$$

where  $dN^{ISM}/dk_{ISM}$  is the differential flux prior to the effects of solar modulation,  $E_{kin}$ ,  $|Z|e$  and  $m$  are the kinetic energy, charge and mass of the cosmic ray, and  $\Phi$  is the modulation potential.

## Modulation Potential

We employ the following modulation potential

$$\Phi(R, t, q) = \phi_0 \left( \frac{|B_{\text{tot}}(t)|}{4 \text{ nT}} \right) + \phi_1 N'(q) H(-qA(t)) \left( \frac{|B_{\text{tot}}(t)|}{4 \text{ nT}} \right) \left( \frac{1 + (R/R_0)^2}{\beta(R/R_0)^3} \right) \left( \frac{\alpha(t)}{\pi/2} \right)^4, \quad (23)$$

- $\beta$  is the velocity.
- $R$  is the rigidity  $R = \sqrt{k_{\text{ISM}}(k_{\text{ISM}} + 2m_p)}$ , and  $R_0 \equiv 0.5 \text{ GV}$ .
- $B_{\text{tot}}$  is the strength of the heliospheric magnetic field (HMF) at Earth, which has a polarity  $A(t)$ .
- $H$  is the heaviside function and  $\alpha$  is tilt angle of the heliospheric current sheet.
- $N'(q) \neq 1$  when the HMF does not have a well-defined polarity.

Parameters according to the AMS-02 measurements (Phys. Rev. D 95, 123007 (2017)).

## Fitting the antiproton-to-proton ratio

To find the differential flux in terms of the kinetic energy measured on Earth ( $E_{\text{kin}}$ ), we obtain the corresponding energy to a given value of  $k_{\text{ISM}}$  by solving

$$E_{\text{kin}} = k_{\text{ISM}} - |Z|e\Phi(R) \quad (24)$$

There is an additional parameter to adjust for the normalization of the ISM gas density,  $g_n$ , that is energy-independent. The flux ratio is defined as follows.

$$R_{\bar{p}/p} = \frac{\Phi_{\bar{p}}}{\Phi_p} = g_n \times \frac{\frac{dN_{\bar{p}}^{\oplus}}{dE_{\text{kin}}}}{\frac{dN_p^{\oplus}}{dE_{\text{kin}}}} \quad (25)$$

Thus, we have six (seven) parameters to fit to the  $\bar{p}/p$  ratio presented by the AMS-02 collaboration:  $\{\phi_0, \phi_1, a, b, c, g_n\}$ .

## Best Fit to the Proton and Antiproton Fluxes (without DM)

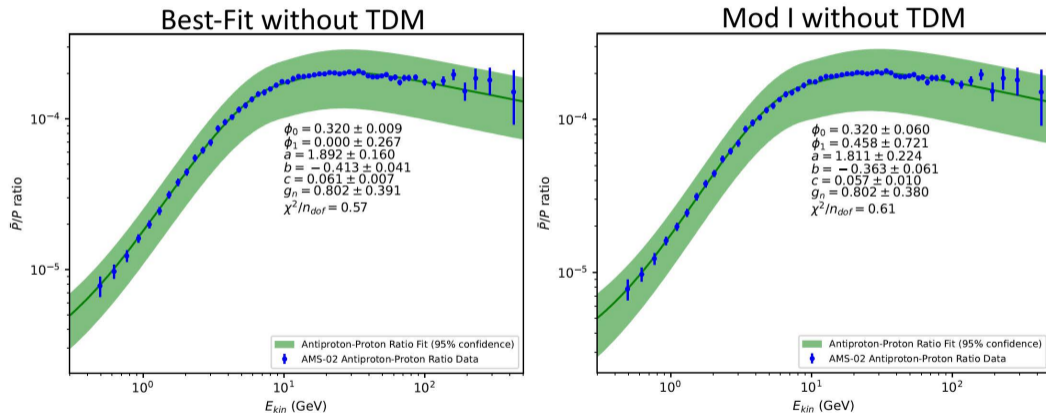


Figura: Best fit to the AMS-02 antiproton-to-proton for the Mod I and our Best-Fit configurations.

## Antiproton-Proton Ratio Residual

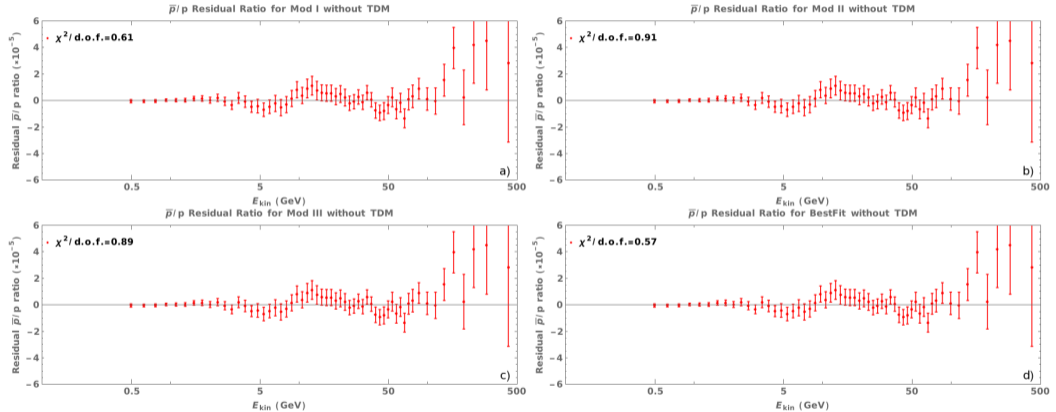
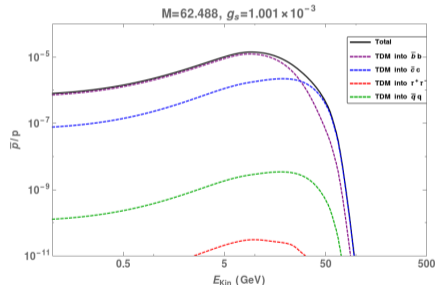


Figura: Antiproton-to-proton ratio residual from the AMS-02 data without TDM for the four parameter configurations.

## Antiproton flux from DM annihilation (prior Solar Modulation)

We use the **PPC4DMID code** (J. Cosmol. Astropart. Phys. 03 (2011) 051).

It obtains the flux produced from hadronization and propagation of DM annihilation products using Monte Carlo simulations, and it includes electroweak corrections.



We do not need to include  $p$  production from DM annihilation, since the contribution to the overall  $p$  flux is negligible to the  $\bar{p}/p$  ratio. Only the  $\bar{p}$  production is large enough to be relevant.



## Best Fit including TDM

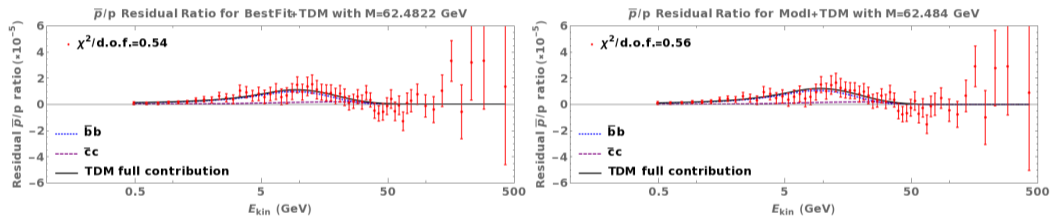
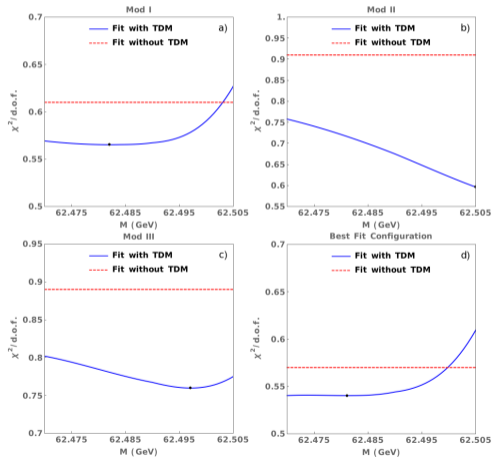


Figura: Antiproton-to-proton ratio pure residual (annihilation contributions not included) from the AMS-02 data for Mod I and our Best-Fit configurations.

## Cosmic-Ray Antiproton Excess: Final Results

The fit improves for almost all values of  $M \in [62.470, 62.505]$  GeV in all configurations.



## Antiproton-To-Proton Ratio Fit with TDM

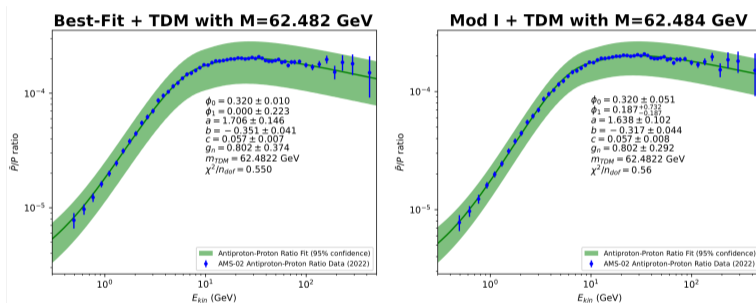


Figura: Antiproton-to-proton ratio fits to the AMS-02 data including the best-fit contributions from TDM annihilation into fermion pairs, for the Mod I and our Best-Fit parameter configurations. The shadowed region corresponds to the 95 % confidence-level.

## AMS-02 Antiproton excess?

- Low energy antiproton cosmic ray spectra affected significantly by uncertainties (production cross-section, propagation, solar modulation, correlations...).
- Comprehensive analyses conclude that data is consistent with **purely secondary origins**, with a global significance of the excess  $\sim 2\sigma$ . (See: Phys.Rev.Res. 2 (2020) 023022, Phys.Rev.Res. 2 (2020) 4, 043017)
- More data, better management of uncertainties might reduce this significance even further.

Model errors and the uncertainties mentioned need to be carefully assessed to reach a conclusion!

However, if handled properly, fits with DM contributions to the antiproton-to-proton ratio can be used to generate bounds on the dark matter model.

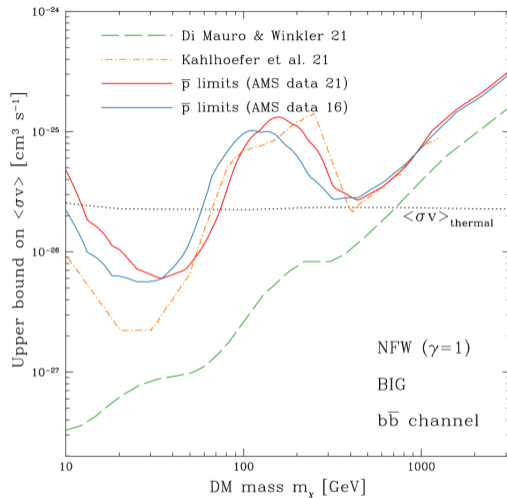


Figura: Upper limit on  $\langle \sigma v \rangle_{b\bar{b}}$  derived from the AMS-02 Antiproton-to-Proton ratio study done by Calore et. al. (SciPost Phys. 12 (2022) 5, 163).

## Conclusions

- We proposed an unconventional  $(1, 0) \oplus (0, 1)$  space-time structure for dark matter: Tensor dark matter.
- The singlet-singlet principle for the effective field theory of SM fields interacting with TDM at leading order yields:
  - 1 A spin portal: coupling of  $\gamma, Z^0$  to higher multipoles of DM.
  - 2 A Higgs portal:  $g_s$  (scalar interactions) and  $g_p$  (pseudoscalar, parity violating interaction).
- Consistency of invisible widths of  $Z^0, H^0$  and DM relic density constrain  $M > 43$  GeV.
- We calculated the relic density for tensor dark matter and comparing with the CMB result, we arrived at a relation between the TDM mass and the coupling constants of the model.
- XENON1T yield stronger constraints on the spin portal coupling  $g_T(M = 200\text{GeV}) \leq 10^{-4}$ , weaker constraints for  $g_s$  and no constraints for  $g_p$ .
- We showed that the gamma ray excess in the Galactic Center can be explained with TDM annihilation for values of the scalar coupling to the Higgs of  $g_s \in [0.98, 1.01] \times 10^{-3}$  and  $M \in [62.470, 62.505]$  GeV.

## Conclusions

- For this mass and coupling window, other experimental observations are successfully explained, such as annihilation into  $\mu^+\mu^-$ ,  $\tau^+\tau^-$  and  $\bar{b}b$  from the measurements of gamma flux of 19 dwarf spheroidal satellite galaxies.
- Such parameters are also consistent with dark matter annihilation into  $\gamma\gamma$  from measurements of monoenergetic spectral lines from self-annihilations of DM in the central region of the Milky Way halo.
- We showed that the inclusion of tensor dark matter annihilating into fermions can improve the fit to the Cosmic-Ray Antiproton Excess from the AMS-02 data, for the mass window consistent with the aforementioned indirect detection limits. However, errors and uncertainties need to be properly assessed for a more robust conclusion.
- Two main challenges for future work: 1) assessing theoretical uncertainties in anti-proton production cross-sections via laboratory measurements and 2) improvement of existing and opening up new cosmic-ray antinuclei channels to further advances on DM constraints.

**THANK YOU!**



## Quantization

Canonical quantization of the theory done in: M. Napsuciale, S. Rodríguez, R. Ferro-Hernández and S. Gómez-Ávila, **Phys. Rev. D** **93** (2016) 076003 [arXiv:1509.07938].

The particle (antiparticle) solutions  $\mathcal{U}(p, \lambda)$  ( $\mathcal{V}(p, \lambda)$ ) satisfy,

$$\sum_{\lambda} \mathcal{U}(p, \lambda) \bar{\mathcal{U}}(p, \lambda) = \sum_{\lambda} \mathcal{V}(p, \lambda) \bar{\mathcal{V}}(p, \lambda) = \frac{S^{\mu\nu} p_{\mu} p_{\nu} + M^2}{2M^2} = \frac{S(p) + M^2}{2M^2} \quad (26)$$

Propagator

$$\Delta(p) = \frac{S(p) - p^2 + 2M^2}{2M^2(p^2 - M^2 + i\epsilon)}$$

## Properties of the operators of the basis in $(1, 0) \oplus (0, 1)$ Representation

$$\{\chi, S^{\mu\nu}\} = 0, \quad \chi^2 = 1, \quad [\chi, \mathcal{O}] = 0, \quad \{S^{\mu\nu}, \chi\} = 0 \quad (27)$$

$$[S^{\mu\nu}, S^{\alpha\beta}] = -i(g^{\mu\alpha}M^{\nu\beta} + g^{\nu\alpha}M^{\mu\beta} + g^{\nu\beta}M^{\mu\alpha} + g^{\mu\beta}M^{\nu\alpha}),$$

$$\{S^{\mu\nu}, S^{\alpha\beta}\} = \frac{4}{3}(g^{\mu\alpha}g^{\nu\beta} + g^{\nu\alpha}g^{\mu\beta} - \frac{1}{2}g^{\mu\nu}g^{\alpha\beta}) - \frac{1}{6}(C^{\mu\alpha\nu\beta} + C^{\mu\beta\nu\alpha}) \quad (28)$$

$$C^{\mu\nu\alpha\beta} + C^{\mu\alpha\beta\nu} + C^{\mu\beta\nu\alpha} = 0, \quad \text{Tr}[C^{\mu\nu\alpha\beta}] = 0 \quad (29)$$

$$\text{Tr}(\chi) = \text{Tr}(S) = \text{Tr}(M) = \text{Tr}(\chi S) = \text{Tr}(C) = 0, \quad (30)$$

$$\begin{aligned} \text{Tr}(\chi M) &= \text{Tr}(\chi C) = \text{Tr}(MS) = \text{Tr}(M\chi S) \\ &= \text{Tr}(MC) = \text{Tr}(S\chi S) = \text{Tr}(SC) = \text{Tr}(\chi SC) = 0. \end{aligned} \quad (31)$$

The particle (antiparticle) solutions  $\mathcal{U}(p, \lambda)$  ( $\mathcal{V}(p, \lambda)$ ) satisfy,

$$\sum_{\lambda} \mathcal{U}(p, \lambda) \bar{\mathcal{U}}(p, \lambda) = \frac{S^{\mu\nu} p_{\mu} p_{\nu} + M^2}{2M^2} = \frac{S(p) + M^2}{2M^2} \quad (32)$$

The free lagrangian for spin-one matter fields is given by,

$$\mathcal{L} = \partial_{\mu} \bar{\Psi} \Sigma^{\mu\nu} \partial_{\nu} \Psi - m^2 [\bar{\Psi} \Psi] \quad (33)$$

where  $\Sigma^{\mu\nu} = \frac{1}{2}(g^{\mu\nu} + S^{\mu\nu})$ .

## Traces

La ortogonalidad de los operadores indica de manera directa las siguientes relaciones.

$$\begin{aligned}\text{Tr}(\chi) &= \text{Tr}(S) = \text{Tr}(M) = \text{Tr}(\chi S) = \text{Tr}(C) = 0, \\ \text{Tr}(\chi M) &= \text{Tr}(\chi C) = \text{Tr}(MS) = \text{Tr}(M\chi S) \\ &= \text{Tr}(MC) = \text{Tr}(S\chi S) = \text{Tr}(SC) = \text{Tr}(\chi SC) = 0.\end{aligned}\tag{34}$$

Además, debido a que  $\{\chi, S^{\mu\nu}\} = 0$ , se tiene que

$$\text{Tr}(\text{cualquier término acompañado de un número de } S \text{ impar}) = 0.$$

Se tienen las siguientes relaciones de conmutación,

$$\begin{aligned}
 [M^{\mu\nu}, M^{\alpha\beta}] &= -i \left( g^{\mu\alpha} M^{\nu\beta} - g^{\nu\alpha} M^{\mu\beta} - g^{\mu\beta} M^{\nu\alpha} + g^{\nu\beta} M^{\mu\alpha} \right) \\
 [M^{\mu\nu}, S^{\alpha\beta}] &= -i \left( g^{\mu\alpha} S^{\nu\beta} - g^{\nu\alpha} S^{\mu\beta} + g^{\mu\beta} S^{\nu\alpha} - g^{\nu\beta} S^{\mu\alpha} \right), \\
 \{M^{\mu\nu}, S^{\alpha\beta}\} &= \varepsilon^{\mu\nu\sigma\beta} \chi S^{\alpha}_{\sigma} + \varepsilon^{\mu\nu\sigma\alpha} \chi S^{\beta}_{\sigma}, \\
 [S^{\mu\nu}, S^{\alpha\beta}] &= -i \left( g^{\mu\alpha} M^{\nu\beta} + g^{\nu\alpha} M^{\mu\beta} + g^{\nu\beta} M^{\mu\alpha} + g^{\mu\beta} M^{\nu\alpha} \right), \\
 \{S^{\mu\nu}, S^{\alpha\beta}\} &= \frac{4}{3} \left( g^{\mu\alpha} g^{\nu\beta} + g^{\nu\alpha} g^{\mu\beta} - \frac{1}{2} g^{\mu\nu} g^{\alpha\beta} \right) - \frac{1}{6} \left( C^{\mu\alpha\nu\beta} + C^{\mu\beta\nu\alpha} \right), \\
 [S^{\mu\nu}, S^{\alpha}_{\nu}] &= -6i M^{\mu\alpha}, \\
 \{S^{\mu\nu}, S^{\alpha}_{\nu}\} &= 6g^{\mu\alpha}, \\
 S^{\mu\nu} S^{\alpha}_{\nu} &= 3(g^{\mu\alpha} - iM^{\mu\alpha}).
 \end{aligned}$$

Definimos los siguientes objetos,

$$T_1^{\alpha\beta\mu\nu\rho\sigma\gamma\delta} = g^{\mu\alpha} S^{\nu\beta\rho\sigma\gamma\delta} - g^{\nu\alpha} S^{\mu\beta\rho\sigma\gamma\delta} + g^{\mu\beta} S^{\nu\alpha\rho\sigma\gamma\delta} - g^{\nu\beta} S^{\mu\alpha\rho\sigma\gamma\delta}, \quad (35)$$

$$T_2^{\mu\nu\alpha\beta\rho\sigma\gamma\delta} = g^{\rho\alpha} M^{\mu\nu\sigma\beta\gamma\delta} + g^{\sigma\alpha} M^{\mu\nu\rho\beta\gamma\delta} + g^{\sigma\beta} M^{\mu\nu\rho\alpha\gamma\delta} + g^{\rho\beta} M^{\mu\nu\sigma\alpha\gamma\delta}, \quad (36)$$

$$T_3^{\mu\nu\rho\sigma\alpha\beta\gamma\delta} = \varepsilon^{\gamma\delta\tau\beta} \left( \varepsilon^{\mu\nu\eta}{}_{\tau} T^{\rho\sigma\alpha}{}_{\eta} + \varepsilon^{\mu\nu\eta\alpha} T^{\rho\sigma}{}_{\tau\eta} \right) \\ + \varepsilon^{\gamma\delta\tau\alpha} \left( \varepsilon^{\mu\nu\eta}{}_{\tau} T^{\rho\sigma\beta}{}_{\eta} + \varepsilon^{\mu\nu\eta\beta} T^{\rho\sigma}{}_{\tau\eta} \right), \quad (37)$$

$$T_4^{\alpha\beta\mu\nu\rho\sigma\gamma\delta} = g^{\rho\mu} S^{\alpha\beta\sigma\nu\gamma\delta} - g^{\sigma\mu} S^{\alpha\beta\rho\nu\gamma\delta} + g^{\rho\nu} S^{\alpha\beta\sigma\mu\gamma\delta} - g^{\sigma\nu} S^{\alpha\beta\rho\mu\gamma\delta}. \quad (38)$$

Las trazas de algunos productos de operadores se muestran a continuación.

$$\text{Tr} \left( M^{\mu\nu} M^{\alpha\beta} \right) = g^{\mu\alpha} g^{\nu\beta} - g^{\mu\beta} g^{\nu\alpha} = 4G^{\mu\nu\alpha\beta},$$

$$\text{Tr} \left( S^{\mu\nu} S^{\alpha\beta} \right) = g^{\mu\alpha} g^{\nu\beta} + g^{\mu\beta} g^{\nu\alpha} - \frac{1}{2} g^{\mu\nu} g^{\alpha\beta} = 4T^{\mu\nu\alpha\beta},$$

$$\text{Tr} \left( S^{\mu\nu} S^{\alpha\beta} M^{\rho\sigma} \right) = -2i(g^{\mu\alpha} G^{\nu\beta\rho\sigma} + g^{\mu\beta} G^{\nu\alpha\rho\sigma} + g^{\nu\alpha} G^{\mu\beta\rho\sigma} + g^{\nu\beta} G^{\mu\alpha\rho\sigma})$$

$$\text{Tr} \left( M^{\mu\nu} M^{\alpha\beta} M^{\rho\sigma} \right) = -2i(g^{\mu\alpha} G^{\nu\beta\rho\sigma} - g^{\nu\alpha} G^{\mu\beta\rho\sigma} - g^{\mu\beta} G^{\nu\alpha\rho\sigma} + g^{\nu\beta} G^{\mu\alpha\rho\sigma})$$

$$\text{Tr} \left( \chi S^{\gamma\delta} S^{\alpha\beta} M^{\mu\nu} \right) = -2 \left( \varepsilon^{\mu\nu\sigma\beta} T^{\gamma\delta\alpha}{}_{\sigma} + \varepsilon^{\mu\nu\sigma\alpha} T^{\gamma\delta\beta}{}_{\sigma} \right)$$

$$\text{Tr} \left( S^{\alpha\beta} M^{\mu\nu} S^{\rho\sigma} M^{\gamma\delta} \right) = T_1^{\alpha\beta\mu\nu\rho\sigma\gamma\delta} + T_2^{\mu\nu\alpha\beta\rho\sigma\gamma\delta} + T_3^{\mu\nu\rho\sigma\alpha\beta\gamma\delta}$$

$$\text{Tr} \left( S^{\alpha\beta} S^{\mu\nu} M^{\rho\sigma} M^{\gamma\delta} \right) = T_1^{\alpha\beta\mu\nu\rho\sigma\gamma\delta} + T_2^{\mu\nu\alpha\beta\rho\sigma\gamma\delta} + T_3^{\mu\nu\rho\sigma\alpha\beta\gamma\delta} + 2T_4^{\alpha\beta\mu\nu\rho\sigma\gamma\delta}.$$

Como ejemplo, el caso más simple de cálculo es el proceso  $H \rightarrow \bar{D}D$ .

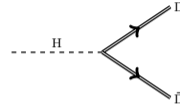
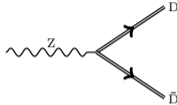
$$\begin{aligned} \text{Tr} \left( S^{\mu\nu} S^{\alpha\beta} \right) &= \text{Tr} \left( \frac{1}{2} [S^{\mu\nu}, S^{\alpha\beta}] + \frac{1}{2} \{S^{\mu\nu}, S^{\alpha\beta}\} \right) \\ &= 4 \left( g^{\mu\alpha} g^{\nu\beta} + g^{\mu\beta} g^{\nu\alpha} - \frac{1}{2} g^{\mu\nu} g^{\alpha\beta} \right) \equiv 4T^{\mu\nu\alpha\beta}. \end{aligned} \quad (39)$$

De la misma forma, es posible realizar el cálculo del proceso  $Z^0 \rightarrow \bar{D}D$ , donde se requiere realizar las siguientes trazas,

$$\begin{aligned} \text{Tr} \left( M^{\mu\nu} M^{\alpha\beta} \right) &= \text{Tr} \left( \frac{1}{2} [M^{\mu\nu}, M^{\alpha\beta}] + \frac{1}{2} \{M^{\mu\nu}, M^{\alpha\beta}\} \right) \\ &= 4(g^{\mu\alpha} g^{\nu\beta} - g^{\mu\beta} g^{\nu\alpha}) \equiv 4G^{\mu\nu\alpha\beta}. \end{aligned} \quad (40)$$



**For low mass:  $Z^0 \rightarrow \bar{D}D$  and  $H \rightarrow \bar{D}D$  decays.**



■ The decay width for these processes are

$$\Gamma_{Z \rightarrow D\bar{D}} = \frac{g_t^2 \sin^2 \theta_W (M_Z^2 - 4M^2)^{3/2}}{24\pi M^4} (M_Z^2 + 2M^2)$$

$$\Gamma_{H \rightarrow D\bar{D}} = \frac{v^2 \sqrt{M_H^2 - 4M^2}}{32\pi M^4 M_H^2} \left[ g_s^2 (M_H^4 - 4M_H^2 M^2 + 6M^4) + g_p^2 M_H^2 (M_H^2 - 4M^2) \right]$$

■ The measured invisible widths of  $Z^0$  and  $H$  are

$$\Gamma_Z^{\text{inv} - \bar{\nu}\nu} = 1.4 \pm 1.5 \text{ MeV. } ^1$$

$$\Gamma_H^{\text{inv}} = 1.14 \pm 0.04 \text{ MeV. } ^2$$

<sup>1</sup>Particle Data Group's Review of Particle Physics.

<sup>2</sup>Khachatryan et al., CMS Coll.; J. High Energy Phys. 02 (2017) 135.

## Upper limits from invisible widths

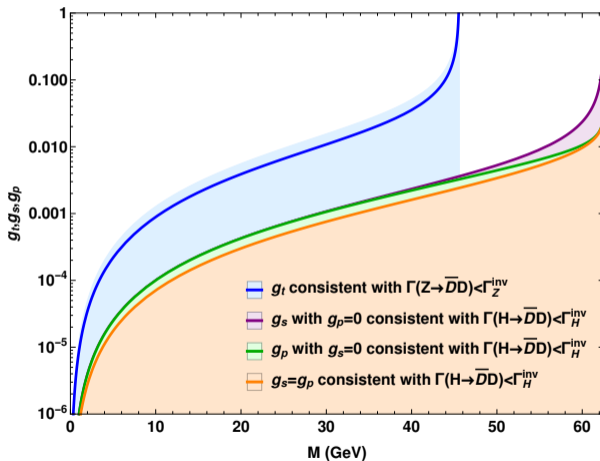
Upper limits for  $g_t$ ,  $g_s$ ,  $g_p$

$$g_t \leq \sqrt{\frac{(1.4)24\pi M^4}{\sin^2\theta_W(M_Z^2 - 4M^2)^{3/2}(M_Z^2 + 2M^2)}}$$

$$g_s \leq \sqrt{\frac{(1.14)32\pi M^4 M_H^2}{v^2 \sqrt{M_H^2 - 4M^2} [M_H^2 (M_H^2 - 4M^2) + 6M^4]}}$$

$$g_p \leq \sqrt{\frac{(1.14)32\pi M^4}{v^2 (M_H^2 - 4M^2)^{3/2}}}$$

## Invisible width constraints on the values of $g_t$ , $g_s$ and $g_p$ .



## Ecuación de Boltzmann

La ecuación de Boltzmann establece que la tasa de cambio en la abundancia de una partícula es la diferencia entre la tasa de producción y la tasa de eliminación de la especie.

$$\frac{df}{dt} = C[f] \quad (41)$$

Podemos escribir esta ecuación en términos de operadores que actúan sobre la función de distribución.

$$L[f] = \left[ \frac{\partial}{\partial t} + \frac{d\vec{x}}{dt} \vec{\nabla}_x + \frac{d\vec{p}}{dt} \vec{\nabla}_p \right] f = C[f] \quad (42)$$

Para la métrica FLRW, el operador de Liouville actuando sobre  $f(E, t)$ , es,

$$L[f(E, t)] = E \frac{\partial}{\partial t} f(E, t) - \frac{\dot{R}}{R} |\vec{p}|^2 \frac{\partial}{\partial E} f(E, t) \quad (43)$$

Utilizando la definición de la densidad numérica en términos de la función de distribución,

$$n(t) = g \int \frac{d^3 p}{(2\pi)^3} f(E, t) \quad (44)$$

E integrando la Ec. (42) en el espacio fase, y dividiendo por la energía del sistema,  $E$ , luego de un poco de desarrollo, se obtiene,

$$R^{-3} \frac{d(R^3 n)}{dt} = g \int \frac{d^3 p}{E(2\pi)^3} C[f(E, t)] \quad (45)$$

## Operador de colisiones

Proceso de aniquilación:  $1 + 2 \longleftrightarrow 3 + 4$

$$g \int \frac{d^3p}{E(2\pi)^3} C[f(E, t)] = - \int d\Pi_1 d\Pi_2 d\Pi_3 d\Pi_4 (2\pi)^4 \delta^4(P_1 + P_2 - P_3 - P_4) \\ \times \left[ |M|_{1+2 \rightarrow 3+4}^2 f_1 f_2 (1 \pm f_3)(1 \pm f_4) - |M|_{3+4 \rightarrow 1+2}^2 f_3 f_4 (1 \pm f_1)(1 \pm f_2) \right] \quad (46)$$

Donde el signo ( $\pm$ ) corresponde a si la partícula es un bosón o un fermión, respectivamente, y  $d\Pi_i = \frac{d^3p}{2E_i(2\pi)^3}$ .

Considerese que el cuadrado del elemento de matriz es invariante ante inversión temporal, de forma que

$$|M|_{1+2 \rightarrow 3+4}^2 = |M|_{3+4 \rightarrow 1+2}^2 = |M|^2 \quad (47)$$

En ausencia de condensación Bose-Einstein, o de degeneración de Fermi, el término  $(1 \pm f_i) \simeq 1$ . De esta forma, tenemos,

$$g \int \frac{d^3p}{E(2\pi)^3} C[f(E, t)] = - \int d\Pi_1 d\Pi_2 d\Pi_3 d\Pi_4 (2\pi)^4 \delta^4(P_1 + P_2 - P_3 - P_4) \\ \times |M|^2 [f_1 f_2 - f_3 f_4] \quad (48)$$

Asumir equilibrio térmico para las especies 3 y 4 es una buena aproximación.

$$f_3 f_4 = (e^{(\mu_3 - E_3)/T})(e^{(\mu_4 - E_4)/T}) \xrightarrow{\delta} (e^{-(E_1 + E_2)/T})(e^{(\mu_3 + \mu_4)/T}) \quad (49)$$

$$f_1 f_2 - f_3 f_4 \xrightarrow{\delta} e^{-(E_1 + E_2)/T} \left[ \frac{n_1 n_2}{n_1^{(0)} n_2^{(0)}} - \frac{n_3 n_4}{n_3^{(0)} n_4^{(0)}} \right] \quad (50)$$

La integral del factor de colisiones es, entonces,

$$\begin{aligned} g \int \frac{d^3 p}{E(2\pi)^3} C[f(E, t)] &= -\frac{g_1 g_2}{n_1^{(0)} n_2^{(0)}} \int d\Pi_1 d\Pi_2 d\Pi_3 d\Pi_4 (2\pi)^4 \\ &\times \delta^4(P_1 + P_2 - P_3 - P_4) e^{-(E_1 + E_2)/T} |M|^2 \end{aligned} \quad (51)$$



## Direct detection of Dark Matter

The rate of interactions of a DM particle of mass  $M$  with a nucleus of mass  $M_A$  in the detector is given by

$$\frac{dR}{dT} = \frac{\rho}{MM_A} \int_{v_{\min}}^{v_{\text{esc}}} |v| f(v) \frac{d\sigma}{dT}(T, v) d^3v, \quad (52)$$

Where  $v_{\min}(T)$  is the minimal velocity of the incoming DM particle to produce a nuclear recoil energy  $T$ , and  $v_{\text{esc}} = 557 \text{ km/s}$  is the escape velocity in our galaxy.

## Boltzmann Equation Solutions

We can solve the equation numerically for a limited range  $x < 10^3$ .

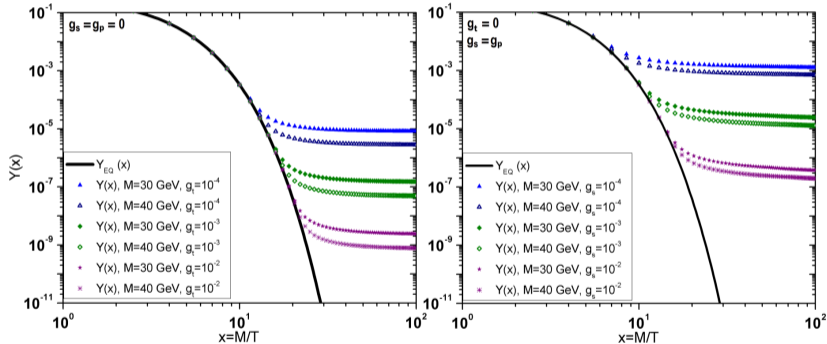


Figura: Solution of the Boltzmann equation for the spin portal (left) and Higgs portal (right). Similar results are obtained in the later case when varying independently  $g_s$  and  $g_p$ . The solid line corresponds to  $Y_{\text{eq}}(x)$ .

## Dark matter relic density: Complete Calculation

From measured branching ratios, we extract the value of the form factors,

$$\text{BR}[H \rightarrow \gamma\gamma] = 2.27 \times 10^{-3} \quad \longrightarrow \quad g_{\gamma\gamma} = 1.91 \times 10^{-3}$$

$$\text{BR}[H \rightarrow Z\gamma] = 1.53 \times 10^{-3} \quad \longrightarrow \quad g_{Z\gamma} = 3.30 \times 10^{-3}$$

These correspond to the form factors for **on-shell momentum**.

The  $\bar{D}D \rightarrow \gamma\gamma, Z^0\gamma$  process via the scalar Higgs portal produces the following cross-sections:

$$(\sigma_{\text{v}_r})_{\gamma\gamma} = \frac{g_{\gamma\gamma}^2 g_s^2 v^2 s^2 (6M^4 - 4M^2s + s^2)}{288\pi M^4 M_H^2 (s - 2M^2) [(s - M_H^2)^2 + M_H^2 \Gamma_H^2]}, \quad (53)$$

$$(\sigma_{\text{v}_r})_{Z\gamma} = \frac{g_{Z\gamma}^2 g_s^2 v^2 (s - M_Z^2)^3 (6M^4 - 4M^2s + s^2)}{144\pi M^4 M_H^2 (s - 2M^2) s [(s - M_H^2)^2 + M_H^2 \Gamma_H^2]}. \quad (54)$$

## DM-Nucleon scattering

$D(p_1)N_A(p_2) \rightarrow D(p_3)N_A(p_4)$  in the LAB system where  $p_1 = (E_1, p_1)$ ,  $p_2 = (M_A, 0)$ ,  $p_3 = (E_3, p_3)$ ,  $p_4 = (M_A + T, p_A)$

$$\frac{d\sigma}{dT}(T, v) = \frac{|\bar{\mathcal{M}}(s, t, u)|^2}{32\pi M_A p_1^2}. \quad (55)$$

The Mandelstam variables in the LAB frame are given by

$$s = (E_1 + M_A)^2 - p_1^2 = (M + M_A)^2 + MM_A v^2 + \mathcal{O}(v^4), \quad (56)$$

$$t = T^2 - |p_A|^2 = -2M_A T, \quad (57)$$

$$u = (M - M_A)^2 + 2M_A T - MM_A v^2 + \mathcal{O}(v^4). \quad (58)$$

For a given incoming momentum  $p_1$ , the nuclear recoil energy is given by

$$T = \frac{2M_A M^2 v^2 \cos^2 \theta}{(E_1 + M_A)^2 - M^2 v^2 \cos^2 \theta} = \frac{2M_A M^2 v^2 \cos^2 \theta}{(M + M_A)^2} + \mathcal{O}(v^4), \quad (59)$$

The minimal velocity  $v_{\min}(T)$  is obtained when  $\theta = 0$ .

$$v_{\min}^2(T) = \frac{(M + M_A)^2}{2M_A M^2} T = \frac{M_A}{2\mu_A^2} T, \quad (60)$$

## Effective theory for nucleus DM interactions

$$\mathcal{M} = \mathcal{M}_0 F_{\text{SI}}(q^2), \quad (61)$$

where  $\mathcal{M}_0$  is calculated with the effective theory at the nuclear level and  $F_{\text{SI}}(q^2)$  is the nucleus form factor.

$$\frac{d\sigma}{dT}(T, \nu) = \frac{|\bar{\mathcal{M}}_0(s, t, u)|^2}{32\pi M_A M^2 \nu^2} F_{\text{SI}}^2(t) = \frac{\xi}{\nu^2} g(T, \nu^2) F_{\text{SI}}^2(T). \quad (62)$$

Expanding for low  $T$ ,

$$\frac{d\sigma}{dT}(T, \nu) \approx \frac{\xi}{\nu^2} g_0(\nu^2) F^2(0). \quad (63)$$

Integrating from 0 to  $T_{\max} = 2\mu_A^2 v^2/M_A$  we obtain

$$\sigma(v) \approx \frac{g_0(v^2)}{32\pi M_A M^2 v^2} \frac{2\mu_A^2 v^2}{M_A} \approx \frac{\mu_A^2 g_0(0)}{16\pi M_A^2 M^2} \equiv \sigma_{\text{SI}}, \quad (64)$$

We can write the actual differential cross section in Eq. (62) to leading order in  $T$  as

$$\frac{d\sigma}{dT}(T, v) = \frac{M_A}{2\mu_A^2 v^2} \sigma_{\text{SI}} F_{\text{SI}}^2(T), \quad (65)$$

The most recent data on direct dark matter detection are given by XENON1T, who assume isospin conserving dark matter-nucleus interactions and report the following observable

$$\sigma_{\text{P}} = \frac{\mu_{\text{P}}^2}{A^2 \mu_A^2} \sigma_{\text{SI}}, \quad (66)$$

In our formalism, the mediators are  $\mathbf{H}$ ,  $Z^0$  and  $\gamma$ . The latter has a propagator with a pole at  $q^2 = 0$ .

**We must modify the relations in order to calculate de XENON1T observable properly.**

Experiments start detecting nuclear recoil at a given  $T = T_{\min}$ :

$$\begin{aligned} \frac{d\sigma}{dT}(T, v) &= \\ & \frac{\xi}{v^2} [g(T_{\min}, v^2) + g'(T_{\min}, v^2)(T - T_{\min})] \\ & \times [F^2(T_{\min}) + (F^2)'(T_{\min})(T - T_{\min})] \\ & = \frac{\xi}{v^2} g(T_{\min}, v^2) F_{\text{SI}}^2(T_{\min}) + \mathcal{O}(T - T_{\min}). \end{aligned} \tag{67}$$



$$\sigma_{\text{SI}} = \frac{\mu_A^2}{16\pi M_A^2 M^2} g(T_{\text{min}}, v^2). \quad (68)$$

The average squared amplitude has the following form

$$g(T, v^2) = a_0 + \left( \frac{b_0}{T} + c_0 \right) v^2 + \mathcal{O}(T, v^4). \quad (69)$$

The observable  $\sigma_P$  reported by XENON is then given by

$$\sigma_P = \frac{1}{16\pi A^4 (M + M_P)^2} \left[ a_0 + \left( \frac{b_0}{T_{\text{min}}} + c_0 \right) v^2 + \mathcal{O}(T, v^4) \right]. \quad (70)$$

## Effective Lagrangian - Higgs Interaction

Quark

$$\mathcal{L}_{Hq\bar{q}} = -\frac{m_q}{v} H\bar{q}q \quad (71)$$

Nucleon

$$\mathcal{L}_{Hq\bar{q}} = C_{HNN} H\bar{N}N \quad (72)$$

$$C_{HNN} = \sum_{u,d,s} \left(-\frac{m_q}{v}\right) \frac{m_N}{m_q} f_{Tq}^{(N)} + \frac{2}{27} f_{TG}^{(N)} \sum_{c,b,t} \left(-\frac{m_q}{v}\right) \frac{m_N}{m_q} \quad (73)$$

$$= -\frac{m_N}{v} \sum_{u,d,s} f_{Tq}^{(N)} - \frac{2}{27} f_{TG}^{(N)} \frac{m_N}{v} \quad (3), \quad (74)$$

Using

$$f_{\text{TG}}^{(N)} = 1 - \sum_{u,d,s} f_{\text{Tq}}^{(N)} \quad (75)$$

We obtain

$$C_{\text{HNN}} = -\frac{m_N}{v} \sum_{u,d,s} f_{\text{Tq}}^{(N)} - \frac{2}{9} \left( 1 - \sum_{u,d,s} f_{\text{Tq}}^{(N)} \right) \frac{m_N}{v} \quad (76)$$

$$= -\left( 7 \sum_{u,d,s} f_{\text{Tq}}^{(N)} + 2 \right) \frac{m_N}{9v} \quad (77)$$

Effective vertex

$$g_{\text{HNN}} = -i \left( 7 \sum_{u,d,s} f_{\text{Tq}}^{(N)} + 2 \right) \frac{m_N}{9v} \quad (78)$$

$$\mathcal{L}_{\text{HNN}} = -ig_{\text{HNN}} H \bar{u}_N u_N \quad (79)$$

## Effective Lagrangian - Photon Interaction

Quark

$$\mathcal{L}_{\gamma q\bar{q}} = -eQ_q A_\mu \bar{q}\gamma^\mu q \quad (80)$$

Nucleon

$$\mathcal{L}_{\gamma NN} = -eQ_N A_\mu \bar{u}_N \gamma^\mu u_N \quad (81)$$

## Effective Lagrangian - Z Interaction

Quark

$$\mathcal{L}_{Zq\bar{q}} = \frac{-M_Z}{2v} A^\mu \bar{q} \gamma_\mu (A_q + B_q \gamma_5) q \quad (82)$$

Nucleon

$$\mathcal{L}_{ZNN} = \frac{-M_Z}{2v} Z^\mu \bar{u}_N \gamma_\mu (A_N + B_N \gamma_5) u_N \quad (83)$$

Where

$$A_p = 2A_u + A_d = 1 - 4 \sin^2 \theta_W \quad (84)$$

$$A_n = A_u + 2A_d = -1 \quad (85)$$

and

$$B_N = -\Delta_u^{(N)} + \Delta_d^{(N)} + \Delta_s^{(N)}, \quad (86)$$

$$B_p = -\Delta_u^{(p)} + \Delta_d^{(p)} + \Delta_s^{(p)}, \quad (87)$$

$$B_n = -\Delta_d^{(p)} + \Delta_u^{(p)} + \Delta_u^{(p)}. \quad (88)$$

[M. Cirelli, E. Del Nobile and P. Panci, JCAP 1310, 019 (2013) [arXiv:1307.5955 [hep-ph]]]

## Nuclear Lagrangian

At the nuclear level, the effective Lagrangian has a similar form

$$\mathcal{L}_{\text{eff}}^A = g_{HN_A N_A} H \bar{N}_A N_A - Ze \bar{N}_A \gamma^\mu N_A A_\mu - \frac{M_Z}{2v} \bar{N}_A \gamma^\mu (A_A + B_A \gamma^5) N_A Z_\mu, \quad (89)$$

with

$$\begin{aligned} g_{HN_A N_A} &= Zg_{Hpp} + (A - Z)g_{Hnn}, \\ A_A &= ZA_p + (A - Z)A_n, \\ B_A &= ZB_p + (A - Z)B_n, \end{aligned} \quad (90)$$

where  $Z$  stands for the atomic number and  $A$  denotes the total number of nucleons inside the nucleus.

## DM-Nuclei interaction

$$D(p_1)N_A(p_2) \rightarrow D(p_3)N_A(p_4)$$

The corresponding contributions are given by

$$-i\mathcal{M}_H = i \frac{g_{DN_A H}}{t - m_H^2} \bar{U}(p_3) (g_S I + i g_P \chi) U(p_1) \bar{N}_A(p_4) N_A(p_2), \quad (91)$$

$$-i\mathcal{M}_\gamma = - \frac{g_{DN_A \gamma}}{t} \bar{U}(p_3) M_{\alpha\beta} (p_1 - p_3)^\beta U(p_1) \bar{N}_A(p_4) \gamma^\alpha N_A(p_2), \quad (92)$$

$$-i\mathcal{M}_Z = \frac{g_{DN_A Z}}{t - M_Z^2} \bar{U}(p_3) M_{\alpha\beta} (p_1 - p_3)^\beta U(p_1) \bar{N}_A(p_4) \gamma^\alpha (A_A + B_A \gamma_5) N_A(p_2), \quad (93)$$

where

$$g_{DN_A H} = -v g_{HN_A N_A}, \quad (94)$$

$$g_{DN_A \gamma} = 2Z e g_t \cos \theta_W, \quad (95)$$

$$g_{DN_A Z} = \frac{M_Z g_t \sin \theta_W}{v}. \quad (96)$$



## Finding $g(T_{\min}, v^2)$

Expanding the average squared amplitude and keeping the leading terms in  $v^2$  and  $T$  we get

$$\begin{aligned}
 |\mathcal{M}|^2 &= \frac{4g_s^2 g_{\text{DNA}}^2 H M_A^2}{m_H^4} + \frac{2g_{\text{DNA}}^2 \gamma}{3M^2} (M^2 - 2M M_A + 3M_A^2) + \frac{16g_s g_{\text{DNA}} \gamma g_{\text{DNA}} H M_A^2}{3M m_H^2} \\
 &+ \left( \frac{4g_{\text{DNA}}^2 \gamma M_A}{3T} - \frac{16A_A g_{\text{DNA}} \gamma g_{\text{DNA}} Z M_A^2}{3M_Z^2} + \frac{8g_s g_{\text{DNA}} \gamma g_{\text{DNA}} H M_A^2}{3M m_H^2} \right. \\
 &\left. - \frac{2g_{\text{DNA}}^2 \gamma M_A}{3M^2} (M - 4M_A) \right) v^2.
 \end{aligned} \tag{97}$$

$$g(T, v^2) = a_0 + \left( \frac{b_0}{T} + c_0 \right) v^2 + \mathcal{O}(T, v^4). \quad (98)$$

$$a_0 = \frac{4g_s^2 g_{\text{DNA}}^2 H M_A^2}{m_H^4} + \frac{2g_{\text{DNA}}^2 \gamma}{3M^2} (M^2 - 2M M_A + 3M_A^2) + \frac{16g_s g_{\text{DNA}} \gamma g_{\text{DNA}} H M_A^2}{3M m_H^2}, \quad (99)$$

$$b_0 = \frac{4g_{\text{DNA}}^2 \gamma M_A}{3}, \quad (100)$$

$$c_0 = -\frac{16A_A g_{\text{DNA}} \gamma g_{\text{DNA}} Z M_A^2}{3M_Z^2} + \frac{8g_s g_{\text{DNA}} \gamma g_{\text{DNA}} H M_A^2}{3M m_H^2} - \frac{2g_{\text{DNA}}^2 \gamma M_A}{3M^2} (M - 4M_A). \quad (101)$$

## Bounds to $\bar{D}D \rightarrow \mu^+\mu^-, \tau^+\tau^-$

⊗ Upper limit for the  $\mu$  channel:  $\langle\sigma v_{\text{r}}\rangle_{\mu^+\mu^-} \leq 8.96 \times 10^{-26} \text{cm}^3/\text{seg}$  for  $M \cong 62.5 \text{ GeV}$ .

L. Bergstrom, T. Bringmann, I. Cholis, D. Hooper and C. Weniger, Phys. Rev. Lett. 111 171101 (2013). arXiv: 1306.3983

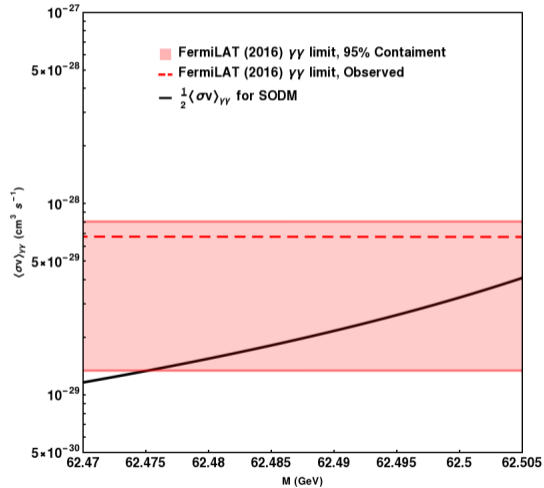
For TDM: Largest value in the GRE-consistent mass region:  $\langle\sigma v_{\text{r}}\rangle_{\mu^+\mu^-} = 8.30 \times 10^{-30} \text{cm}^3/\text{seg}$  for  $M \cong 62.505 \text{ GeV}$  and  $g_{\text{s}} = 9.81 \times 10^{-4}$ .

⊗ Upper limit for the  $\tau$  channel:  $\langle\sigma v_{\text{r}}\rangle_{\mu^+\mu^-} \leq 1.2 \times 10^{-26} \text{cm}^3/\text{seg}$  for  $M \cong 62.5 \text{ GeV}$ .

DES, Fermi-LAT collaboration, Astrophys. J. 809 L4 (2015). arXiv: 1503.02632

For TDM: Largest value in the GRE-consistent mass region:  $\langle\sigma v_{\text{r}}\rangle_{\mu^+\mu^-} = 2.42 \times 10^{-27} \text{cm}^3/\text{seg}$  for  $M \cong 62.505 \text{ GeV}$  and  $g_{\text{s}} = 9.81 \times 10^{-4}$ .

## Other constraints: $\gamma\gamma$ limits



### $3\sigma$ uncertainty on $\sigma_{pp \rightarrow X + \bar{p}}$

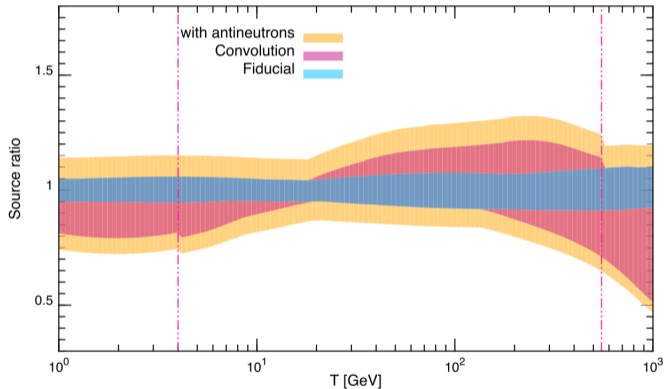


Figura: Estimate of uncertainties in the antiproton source term from inelastic proton-proton scattering. (Phys. Rev. D 90, 085017 (2014)).

## Modelling the antiproton and proton spectrum with GALPROP

GALPROP takes care of solving the transport equation to yield the local flux of the primary and secondary cosmic ray species, which can be written as:

$$\frac{\partial \psi(\vec{r}, p, t)}{\partial t} = Q(\vec{r}, p, t) + \vec{\nabla} \cdot (D_{xx} \vec{\nabla} \psi - \vec{V} \psi) + \frac{\partial}{\partial p} p^2 D_{pp} \frac{\partial}{\partial p} \frac{1}{p^2} \psi - \frac{\partial}{\partial p} \left[ \dot{p} \psi - \frac{p}{3} (\vec{\nabla} \cdot \vec{V}) \psi \right] - \frac{1}{\tau_f} \psi - \frac{1}{\tau_r} \psi, \quad (102)$$

- $\psi(\vec{r}, p, t)$  is the cosmic ray density per unit of particle momentum  $p$  at position  $\vec{r}$ .
- $Q(\vec{r}, p, t)$  is the source term which includes the source injection spectrum (assumed to be radially distributed e.g. supernova remnants) and contribution from spallation.
- $\vec{V}$  is the convection velocity.
- Last two terms involve momentum loss by fragmentation (with time scale  $\tau_f$ ) and from radioactive decay (with time scale  $\tau_r$ ).

## Modelling the antiproton and proton spectrum with GALPROP

Acceleration due to injection in general can be parametrized to the cosmic-ray rigidity  $R$  by a power-law spectrum

$$dN/dR \sim R^{-\alpha} \quad (103)$$

, where  $\alpha$  is called nucleus injection index. Generally, such spectrum can have breaks at rigidity  $R_{\text{br}}$ , with  $\alpha = \alpha_1$  below this value and  $\alpha = \alpha_2$  above it.

The spatial diffusion coefficient is defined by

$$D_{\text{xx}}(R) = \beta D_0 (R/4 \text{ GV})^\delta, \quad (104)$$

where  $\delta$  is the diffusion index and  $\beta \equiv v/c$ . The momentum diffusion coefficient,  $D_{\text{pp}}$ , is inversely proportional to  $D_{\text{xx}}$  and proportional to the squared Alfvén velocity  $v_A$ .

## Six-month average values of the parameters of $\phi(R, t, q)$

PHYSICAL REVIEW D **95**, 123007 (2017)

TABLE II. The values of  $|B_{\text{tot}}|$  and  $\alpha$  as averaged over each six-month interval within the period of AMS-02 observations (May, 2011–May, 2015). We also list the values of  $N'(q) \cdot H(-qA(t))$ , as appearing in Eq. (3), for both protons and antiprotons.

Era	$ B_{\text{tot}} $ (nT)	$\alpha$ (degrees)	$N'(q > 0) \cdot$ $H(-qA(t))$	$N'(q < 0) \cdot$ $H(-qA(t))$
07–12/11	4.7	60.5	1	0
01–06/12	4.8	67.2	1	0
07–12/12	5.3	70.0	0.67	0.33
01–06/13	5.5	71.0	0.50	0.50
07–12/13	5.2	70.0	0.33	0.67
01–06/14	5.3	67.0	0	1
07–12/14	5.6	62.0	0	1
01–06/15	6.6	56.6	0	1



The value of the Fermi constant is extracted from measurements of the muon life-time and its value is related to the physical weak angle by the SM-inspired relation

$$G_F \equiv \frac{\pi\alpha}{\sqrt{2}M_Z^2 c_w^2 s_w^2}, \quad (105)$$

which means the physical weak angle is given in terms of the primary parameters by

$$c_w^2 s_w^2 = \frac{\pi\alpha}{\sqrt{2}G_F M_Z^2}. \quad (106)$$

Similarly, calculating muon decay in the extended theory we can write

$$\hat{c}_w^2 \hat{s}_w^2 = \frac{\pi\alpha}{\sqrt{2}G_F M_Z^2}. \quad (107)$$

Combining these relations we get

$$M_Z^2 c_w^2 s_w^2 = M_Z^2 \hat{c}_w^2 \hat{s}_w^2. \quad (108)$$

## Effects beyond the SM

This relation allows us write

$$\rho_0 \equiv \frac{M_W^2}{c_w^2 M_Z^2} = \frac{s_w^2}{\hat{s}_w^2}. \quad (109)$$

Defining the  $\rho_0^{\text{BSM}}$  parameter which measures the deviation of the SM value as

$$\rho_0^{\text{BSM}} \equiv \frac{M_W^2}{\hat{c}_Z^2 M_Z^2 \hat{\rho}}, \quad (110)$$

where  $\hat{c}_Z^2 \equiv \cos^2 \theta_w(M_Z^2)$  and  $\hat{\rho} = 1.01019 \pm 0.00009$  is the conventional SM rho parameter.

The above value yields  $\rho_0 = \rho_0^{\text{BSM}} \hat{\rho} = 1.010573 \pm 0.000029 = 1 + \delta > 1$ .

## The implications of the global fit to EWPD

We can write the ratios  $\tau$  and  $\sigma$  entirely in terms of physical quantities  $M_W$ ,  $\theta_w$ ,  $M_{Z'}$  and  $M_Z$

$$\tau = \rho_0 \frac{c_w^2}{\hat{c}_w^2} = \frac{\rho_0^2 c_w^2}{\rho_0 - s_w^2}, \quad \sigma = \sigma_0 \frac{c_w^2}{\hat{c}_w^2} = \frac{\sigma_0 \rho_0 c_w^2}{\rho_0 - s_w^2}, \quad (111)$$

where

$$\sigma_0 \equiv \frac{M_W^2}{c_w^2 M_{Z'}^2}. \quad (112)$$

Using these relations, we rewrite  $s_z^2$  in terms of physical quantities  $M_W$ ,  $c_w$ ,  $M_{Z'}$ ,

$$s_z^2 = \frac{(1 - 2s_w^2 + c_w^2 \delta) \sigma_0 \delta}{(1 - \sigma_0 + \delta)(c_w^2 + \delta)}. \quad (113)$$

The condition  $s_z^2 \geq 0$  and the result  $\delta > 0$  from the global fit to EWPD yields  $\sigma_0 < \rho_0$ , i.e.

$$M_{Z'} > M_Z. \quad (114)$$

## Dark Gauge Group

**Hidden Tensor Dark Matter gauge structure.**

**Simplest case:** an additional **dark gauge group**  $G_d = U(1)_d$ .

$$\mathcal{L} = \mathcal{L}_{\text{SM}} + \mathcal{L}_d + \mathcal{L}_{\text{int}}, \quad (115)$$

where the dark sector is given by

$$\mathcal{L}_d = (D^\mu \tilde{\psi})^\dagger \bar{\psi} \Sigma^{\mu\nu} D_\nu \psi - M^2 \bar{\psi} \psi + (D^\mu \Phi)^* D_\mu \Phi - \mu_d^2 \Phi^* \Phi - \lambda_d (\Phi^* \Phi)^2 - \frac{1}{4} V^{\mu\nu} V_{\mu\nu}, \quad (116)$$

with  $\Sigma_{\mu\nu} = \frac{1}{2}(g_{\mu\nu} + S_{\mu\nu})$  and  $D_\mu \psi = (\partial_\mu + ig_d \frac{Q_d}{2} V_\mu) \psi$ .

## Kinetic Mixing

The interaction Lagrangian is given by

$$\begin{aligned} \mathcal{L}_{\text{int}} = & -\bar{\psi}(g_s + ig_p\chi)\psi\hat{\phi}^\dagger\hat{\phi} + g_t\bar{\psi}M_{\mu\nu}\psi\tilde{B}^{\mu\nu} - \bar{\psi}(\tilde{g}_s + i\tilde{g}_p\chi)\psi\Phi^*\Phi \\ & - \frac{\sin\chi}{2}\tilde{B}^{\mu\nu}V_{\mu\nu} - 2\kappa\tilde{\phi}^\dagger\tilde{\phi}\Phi^*\Phi + \mathcal{L}_{\text{si}}^\psi, \end{aligned} \quad (117)$$

where  $\mathcal{L}_{\text{si}}^\Psi$  stands for the self-interaction Lagrangian of tensor dark matter.

From here we see an additional term to the kinetic Lagrangian for the gauge fields

$$\mathcal{L}_{\text{gauge}}^{\text{K}} = -\frac{1}{4}(\hat{W}^{a\mu\nu}\hat{W}_{\mu\nu}^a + \hat{B}^{\mu\nu}\hat{B}_{\mu\nu} + \hat{V}^{\mu\nu}\hat{V}_{\mu\nu} + 2\sin\chi\hat{V}^{\mu\nu}\hat{B}_{\mu\nu}) \quad (118)$$

Normalizing the Lagrangian requires redefinition of the fields by the following  $GL(2, \mathbb{R})$  transformation to recover the canonical form

$$\hat{B}_{\mu\nu} = \bar{B}_{\mu\nu} - \tan\chi\bar{V}_{\mu\nu}, \quad \hat{V}_{\mu\nu} = \sec\chi\bar{V}_{\mu\nu}, \quad (119)$$

## Gauge bosons

The covariant derivative becomes

$$D^\mu = \partial^\mu + i\tilde{g}T^a\tilde{W}^{a\mu} + i\tilde{g}_Y\frac{Y}{2}\tilde{B}^\mu + i(g_d \sec\chi\frac{Q_d}{2} - \tilde{g}_Y \tan\chi\frac{Y}{2})\tilde{V}^\mu. \quad (120)$$

Here, the field  $\tilde{B}^\mu$  is the part of the SM hypercharge field  $\tilde{B}^\mu$  that mixes with  $\tilde{W}^{3\mu}$ , such that we find the physical photon field  $A$  and a massive boson  $\tilde{Z}$ :

$$\begin{pmatrix} \tilde{B} \\ \tilde{W}_3 \end{pmatrix} = \begin{pmatrix} \cos\tilde{\theta}_w & -\sin\tilde{\theta}_w \\ \sin\tilde{\theta}_w & \cos\tilde{\theta}_w \end{pmatrix} \begin{pmatrix} A \\ \tilde{Z} \end{pmatrix}. \quad (121)$$

As a result, we get the relation

$$\tilde{g}T_3\tilde{W}_3 + \tilde{g}_Y\frac{Y}{2}\tilde{B} = eQA + \frac{\tilde{g}}{\tilde{c}_w}(T_3 - \tilde{s}_w^2Q)\tilde{Z}, \quad (122)$$

with  $e = \tilde{g}\tilde{s}_w = \tilde{g}_Y\tilde{c}_w$ , and where  $\tilde{s}_w = \sin\tilde{\theta}_w$ ,  $\tilde{c}_w = \cos\tilde{\theta}_w$ .

## Higgs sector

The Higgs sector of the  $G_{\text{SM}} \otimes U(1)_d$  gauge theory has the following Lagrangian

$$\mathcal{L}_{\text{Higgs}} = (D^\mu \tilde{\phi})^\dagger D_\mu \tilde{\phi} + (D^\mu \Phi)^* D_\mu \Phi - V(\tilde{\phi}, \Phi), \quad (123)$$

where the Higgs potential is written as

$$V(\tilde{\phi}, \Phi) = \tilde{\mu}^2 \tilde{\phi}^\dagger \tilde{\phi} + \tilde{\lambda} (\tilde{\phi}^\dagger \tilde{\phi})^2 + \mu_d^2 \Phi^* \Phi + \lambda_d (\Phi^* \Phi)^2 + 2\kappa \Phi^* \Phi \tilde{\phi}^\dagger \tilde{\phi}. \quad (124)$$

The conditions from SSB give the following relations

$$\mu^2 + \lambda v^2 + \kappa \tilde{v}^2 = 0, \quad \tilde{\mu}^2 + \tilde{\lambda} \tilde{v}^2 + \kappa v^2 = 0, \quad (125)$$

where  $\langle 0 | \phi^\dagger \phi | 0 \rangle = v^2/2$  and  $\langle 0 | \Phi^* \Phi | 0 \rangle = \tilde{v}^2/2$ . The Higgs fields in the unitary gauge are

$$\tilde{\phi} = \begin{pmatrix} 0 \\ \frac{\tilde{v} + \tilde{H}}{\sqrt{2}} \end{pmatrix}, \quad \Phi = \frac{v_d + \bar{S}}{\sqrt{2}}. \quad (126)$$

## Neutral bosons

SSB gives the following gauge boson mass terms

$$\begin{aligned} \mathcal{L}_{\text{mass}}^{\text{gauge}} = & \frac{\tilde{g}^2 \tilde{v}^2}{4} \tilde{W}^{+\mu} \tilde{W}_{\mu}^{-} \\ & + \frac{1}{2} \left[ \frac{\tilde{v}^2 \tilde{g}^2}{4\tilde{c}_w^2} \tilde{Z}^2 + \frac{\tilde{v}^2 \tilde{g} \tilde{g}_Y \tan \chi}{2\tilde{c}_w} \tilde{V}^{\mu} \tilde{Z}_{\mu} + \left( \frac{\tilde{g}_Y^2 \tilde{v}^2 \tan^2 \chi}{4} + g_d^2 \sec^2 \chi v^2 \right) \tilde{V}^2 \right]. \end{aligned} \quad (127)$$

The neutral gauge boson mass terms can be diagonalized by the following rotation

$$\begin{pmatrix} \tilde{Z} \\ \tilde{V} \end{pmatrix} = \begin{pmatrix} \cos \theta_{\zeta} & -\sin \theta_{\zeta} \\ \sin \theta_{\zeta} & \cos \theta_{\zeta} \end{pmatrix} \begin{pmatrix} Z \\ Z' \end{pmatrix}, \quad (128)$$

in which we have the relations

$$M_Z^2 = M_Z^2 c_{\zeta}^2 + M_V^2 s_{\zeta}^2 + 2\Delta s_{\zeta} c_{\zeta}, \quad (129)$$

$$M_{Z'}^2 = M_Z^2 s_{\zeta}^2 + M_V^2 c_{\zeta}^2 - 2\Delta s_{\zeta} c_{\zeta}, \quad (130)$$

$$\tan 2\theta_{\zeta} = \frac{2\Delta}{M_Z^2 - M_V^2}. \quad (131)$$



## Kinetic mixing: full transformation

After these transformations, we can find the relation between the original gauge fields and the diagonal fields by

$$\begin{pmatrix} \tilde{B} \\ \tilde{W}_3 \\ V \end{pmatrix} = \begin{pmatrix} \tilde{c}_w, & -\tilde{s}_w c_\zeta - \tan \chi s_\zeta, & \tilde{s}_w s_\zeta - \tan \chi c_\zeta \\ \tilde{s}_w & \tilde{c}_w c_\zeta & -\tilde{c}_w s_\zeta \\ 0 & \sec \chi s_\zeta & \sec \chi c_\zeta \end{pmatrix} \begin{pmatrix} A \\ Z \\ Z' \end{pmatrix}. \quad (132)$$

Finally, the covariant derivative in terms of the physical fields is

$$\begin{aligned} D_\mu &= \partial_\mu + i \frac{\tilde{g}}{\sqrt{2}} (T^+ \tilde{W}_\mu^+ + T^- \tilde{W}_\mu^-) + ieQA_\mu \\ &+ i \left[ \frac{\tilde{g}c_\zeta}{\tilde{c}_w} \left( (T_3 - \tilde{s}_w^2 Q) - \tilde{s}_w \tan \theta_\zeta \tan \chi \frac{Y}{2} \right) + g_d s_\zeta \sec \chi \frac{Q_d}{2} \right] Z_\mu \\ &- i \left[ \frac{\tilde{g}s_\zeta}{\tilde{c}_w} \left( (T_3 - \tilde{s}_w^2 Q) + \frac{\tilde{s}_w \tan \chi}{\tan \theta_\zeta} \frac{Y}{2} \right) - g_d c_\zeta \sec \chi \frac{Q_d}{2} \right] Z'_\mu. \end{aligned} \quad (133)$$

## Rewriting the parameters in terms of physical masses

- Custodial symmetry protects:  $M_{\tilde{W}} = M_Z \tilde{c}_W$  at tree level.
- Write the parameters of the mixing matrix in terms of  $\theta_W$ ,  $M_W$ ,  $M_Z$  and  $M_{Z'}$ .

$$M_W^2 = \frac{\pi\alpha}{\sqrt{2}G_F\hat{s}_Z^2(1 - \Delta\hat{f}_W)}, \quad M_Z^2 = \frac{M_W^2}{\hat{\rho}\hat{c}_Z^2}, \quad (134)$$

- $\Delta\hat{f}_W$ ,  $\hat{\rho}$  are related to the radiative corrections.
- Including all bosonic loops, we obtain  $\hat{\rho} = 1 + \hat{\rho}_{tb} + \hat{\rho}_H = 1.01019 \pm 0.00009$ .
- The global fit to the EWPD measures effects of new physics

$$\rho_0 \equiv \frac{M_W^2}{\hat{c}_Z^2 M_{Z'}^2 \hat{\rho}} = 1.00038 \pm 0.00020. \quad (135)$$

- We define a new term

$$\sigma_0 \equiv \frac{M_{\tilde{W}}^2}{\hat{c}_Z^2 M_{Z'}^2 \hat{\rho}}. \quad (136)$$

The covariant derivative in terms of the physical measured parameters is

$$\begin{aligned}
 D_\mu = & \partial_\mu + i \frac{e\sqrt{\rho_0}}{\sqrt{2}\hat{s}_Z} (T^+ W_\mu^+ + T^- W_\mu^-) + ieQA_\mu \\
 & + i \left[ \frac{e}{\hat{s}_Z \hat{c}_Z} \sqrt{\frac{\rho_0 - \hat{s}_Z^2 - \rho_0 \sigma_0 \hat{c}_Z^2}{\hat{c}_Z^2 \rho_0 (\rho_0 - \sigma_0)}} (T_3 - (1 - \rho_0 \hat{c}_Z^2)Q) + g_d \hat{s}_\zeta \sec \hat{\chi} \frac{Q_d}{2} \right] Z_\mu \\
 & - i \left[ \frac{e}{\hat{s}_Z \hat{c}_Z} \sqrt{\frac{(\rho_0 - 1)(\rho_0 \hat{c}_Z^2 - \hat{s}_Z^2)}{\hat{c}_Z^2 \sigma_0 (\rho_0 - \sigma_0)}} (T_3 - (1 - \sigma_0 \hat{c}_Z^2)Q) - g_d \hat{c}_\zeta \sec \hat{\chi} \frac{Q_d}{2} \right] Z'_\mu, \tag{137}
 \end{aligned}$$

where

$$\hat{c}_\zeta^2 = \frac{\rho_0(\rho_0 - \hat{s}_Z^2 - \rho_0 \sigma_0 \hat{c}_Z^2)}{(\rho_0 - \hat{s}_Z^2)(\rho_0 - \sigma_0)}, \tag{138}$$

$$\hat{s}_\zeta \sec \hat{\chi} = \frac{1}{\rho_0 \hat{s}_Z \hat{c}_Z^2} \left[ \frac{(\rho_0 - 1)(\rho_0 \hat{c}_Z^2 - \hat{s}_Z^2)(\rho_0(\rho_0 \hat{c}_Z^2 - 1)(1 - \sigma_0 \hat{c}_Z^2) + \hat{s}_Z^2)}{\rho_0 - \sigma_0} \right]^{\frac{1}{2}}, \tag{139}$$

$$\hat{c}_\zeta \sec \hat{\chi} = \frac{1}{\hat{s}_Z \hat{c}_Z} \left[ \frac{\rho_0 - \hat{s}_Z^2 - \rho_0 \sigma_0 \hat{c}_Z^2}{\rho_0 - \sigma_0} \left( \frac{(\rho_0 - 1)(\rho_0(1 - \sigma_0) \hat{c}_Z^2 - \hat{s}_Z^2)}{\sigma_0} + \rho_0 \hat{s}_Z^2 \right) \right]^{\frac{1}{2}}, \tag{140}$$

with  $\hat{c}_\zeta = c_\zeta(M_Z)$ .

## $Z\bar{f}f$ interactions and oblique parameters

The oblique parameters S, T and U can be extracted by comparing the  $Z\bar{f}f$  interaction with its effective Lagrangian read as

$$\mathcal{L}_{Z\bar{f}f}^{\text{eff}} = \frac{e}{2s_W c_W} \left(1 + \frac{\alpha T}{2}\right) \sum_f \bar{f} \gamma^\mu \left(T_{f_L}^3 - 2s_*^2 Q - T_{f_L}^3 \gamma^5\right) f Z_\mu, \quad (141)$$

where  $s_W = \sin \theta_W$ ,  $c_W = \cos \theta_W$  with  $\theta_W$  being the Weinberg angle and

$$s_*^2 = s_W^2 + \frac{1}{c_W^2 - s_W^2} \left(\frac{\alpha S}{4} - s_W^2 c_W^2 \alpha T\right). \quad (142)$$

For HTDM we have the following  $Z\bar{f}f$  Lagrangian

$$\mathcal{L}_{Z\bar{f}f} = \frac{e}{2\hat{s}_Z \hat{c}_Z} R \sum_f \bar{f} \gamma^\mu \left[T_{f_L}^3 - 2(1 - \rho_0 \hat{c}_Z^2) Q - T_{f_L}^3 \gamma^5\right] f Z_\mu, \quad (143)$$

with

$$R = \sqrt{\frac{\rho_0 - s_w^2 - \rho_0 \sigma_0 c_w^2}{c_w^2 \rho_0 (\rho_0 - \sigma_0)}}. \quad (144)$$

## S and T parameters

Comparing both Lagrangians we can identify

$$\alpha S = 4\hat{c}_Z^2 [(1 - \rho_0)(\hat{c}_Z^2 - \hat{s}_Z^2) + 2\hat{s}_Z^2(R - 1)], \quad (145)$$

$$\alpha T = 2(R - 1). \quad (146)$$

The parameters S and T are functions of the  $Z'$  mass, but they are also related by the expression

$$T = \frac{1}{4\hat{s}_Z^2\hat{c}_Z^2} S + (\rho_0 - 1) \frac{\hat{c}_Z^2 - \hat{s}_Z^2}{\alpha\hat{s}_Z^2}, \quad (147)$$

valid for all values of  $M_{Z'}$ .

The values extracted from the fit to EWPD for the oblique parameters are

$$S = -0.01 \pm 0.10, \quad T = 0.03 \pm 0.12, \quad U = 0.02 \pm 0.11. \quad (148)$$

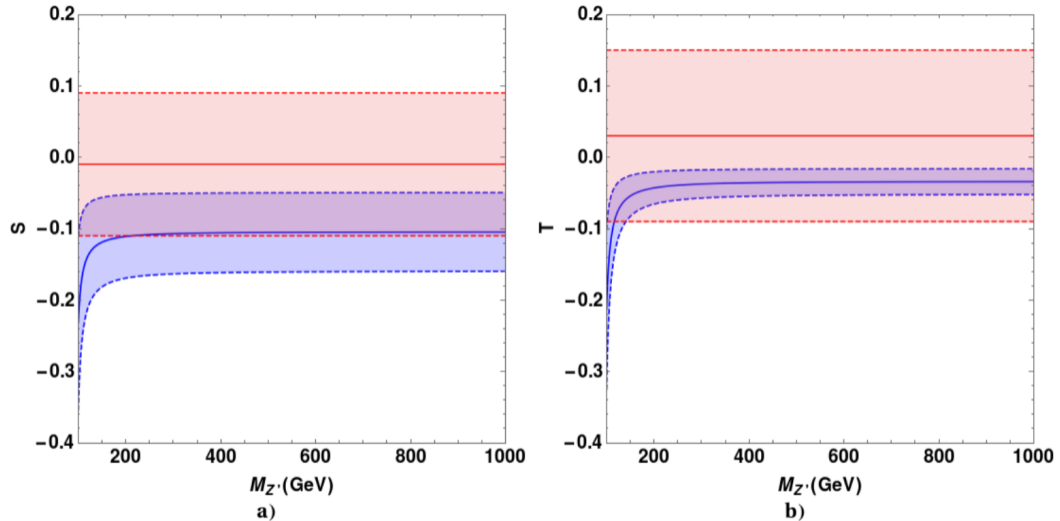


Figura: Oblique parameters  $S$  and  $T$  as functions of  $M_{Z'}$ . The solid blue lines are the predictions using the central value of  $\rho_0$ , while the shadowed band comes from the  $1\sigma$  region for  $\rho_0$ . The red bands correspond to the  $1\sigma$  region for  $S$  and  $T$  from the EWDD fit.

## Z' production at hadron colliders

In the case that SM fermions do not carry the  $U(1)_V$  charges, we have the following  $Z'\bar{f}f$  interactions

$$\mathcal{L}_{Z'\bar{f}f} = g_{Z'} \sum_f \bar{f} \gamma^\mu \left[ T_{f_L}^3 - 2(1 - \sigma_0 \hat{c}_Z^2) Q_f - T_{f_L}^3 \gamma^5 \right] f Z'_\mu, \quad (149)$$

where

$$g_{Z'} = \frac{e}{2\hat{s}_Z \hat{c}_Z} \sqrt{\frac{(\rho_0 - 1)(\rho_0 \hat{c}_Z^2 - \hat{s}_Z^2)}{\hat{c}_Z^2 \sigma_0 (\rho_0 - \sigma_0)}}. \quad (150)$$

In general, the interacting Lagrangian is written as

$$\mathcal{L}_{Z'\bar{f}f} = g' Z'_\mu \sum_f \bar{f} \gamma^\mu [g_V - g_A \gamma^5] f, \quad (151)$$

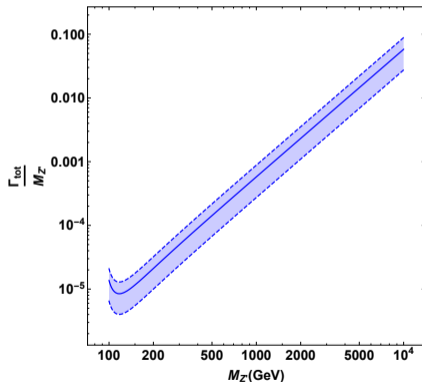
This yields the coupling  $g' = g_{Z'}$  and the following vector and axial factors

$$g_V^f = T_f^3 - 2(1 - \sigma_0 c_w^2) Q_f, \quad g_A^f = T_f^3. \quad (152)$$

We can calculate the total  $Z'$  decay width into SM fermions

$$\Gamma_{Z'}^f = \frac{\alpha M_{Z'}}{4\hat{s}_Z^2 \hat{c}_Z^2} \frac{(\rho_0 - 1)(\rho_0 \hat{c}_Z^2 - \hat{s}_Z^2)}{\hat{c}_Z^2 \sigma_0 (\rho_0 - \sigma_0)} \left[ 1 - 2(1 - \sigma_0 \hat{c}_Z^2) + \frac{8}{3}(1 - \sigma_0 \hat{c}_Z^2)^2 \right]. \quad (153)$$

In a first approximation we will assume that the total width of the  $Z'$  is given by its decays to SM fermions only.



Search of  $Z'$  in the LHC assumes that it will be visible  $\rightarrow \Gamma_{Z'}/M_{Z'} < 1$



## Charged lepton pair production

At leading order the cross section can be written as

$$\sigma_{l^+l^-} = \frac{\pi}{48s} [c_u w_u(s, M_{Z'}^2) + c_d w_d(s, M_{Z'}^2)] \quad (154)$$

where  $w_{u,d}(s, M_{Z'}^2)$  are related to the parton luminosities and the coefficients  $c_{u,d}$  depend on the  $Z'$  couplings to fermions as

$$c_u = \frac{g'^2}{2} [(g_V^u)^2 + (g_A^u)^2] \text{BR}(Z' \rightarrow l^+l^-), \quad (155)$$

$$c_d = \frac{g'^2}{2} [(g_V^d)^2 + (g_A^d)^2] \text{BR}(Z' \rightarrow l^+l^-). \quad (156)$$

## $c_u$ and $c_d$ for large $Z'$ mass

The branching ratio for the  $l^+l^-$  channel is obtained as

$$\text{BR}(Z' \rightarrow l^+l^-) = \frac{1}{8} \frac{1 - 4(1 - \sigma_0 c_w^2) + 8(1 - \sigma_0 c_w^2)^2}{3 - 6(1 - \sigma_0 c_w^2) + 8(1 - \sigma_0 c_w^2)^2}. \quad (157)$$

For large  $Z'$  mass, the branching ratio reaches a saturation value  $\text{BR}(l^+l^-) = 1/8$ . In this limit the  $c_{u,d}$  couplings grow like  $M_{Z'}^2$ ,

$$c_u \approx \frac{17}{8} \frac{\pi \alpha}{36 s_w^2 c_w^2} \frac{(\rho_0 c_w^2 - s_w^2)}{\rho_0} \frac{(\rho_0 - 1)}{c_w^2 \sigma_0} = 1.67 \times 10^{-6} \frac{M_{Z'}^2}{M_W^2}, \quad (158)$$

$$c_d \approx \frac{5}{8} \frac{\pi \alpha}{36 s_w^2 c_w^2} \frac{(\rho_0 c_w^2 - s_w^2)}{\rho_0} \frac{(\rho_0 - 1)}{c_w^2 \sigma_0} = 4.9 \times 10^{-7} \frac{M_{Z'}^2}{M_W^2}. \quad (159)$$

Experimental data on the upper bounds for  $Z'$  production at CMS has been translated into exclusion curves in the  $c_d - c_u$  plane for given values of  $M_{Z'}$ .

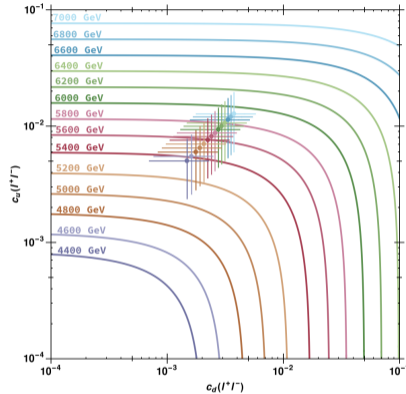


Figura: Exclusion curves for the  $c_u, c_d$  couplings extracted from JHEP 07 (2021) 208 [2103.02708] and the corresponding predictions for this work.

$M_{Z'} < 5200$  GeV is excluded by these bounds in this case.

## Inclusion of TDM field $\psi$ with $U(1)_d$ charge $Q_d^\psi = 2$

We obtain the following decay width

$$\Gamma(Z' \rightarrow \bar{\psi}\psi) = \frac{\alpha_d \hat{c}_\zeta^2 \sec^2 \hat{\chi} M_{Z'}^2}{96M^4} (M_{Z'}^2 - 4M_\psi^2)^{3/2} \left[ 1 - 6 \left( \frac{M_\psi}{M_{Z'}} \right)^2 + 24 \left( \frac{M_\psi}{M_{Z'}} \right)^4 \right], \quad (160)$$

where  $\alpha_d = g_d^2/4\pi$  is the  $U(1)_d$  fine structure constant.

